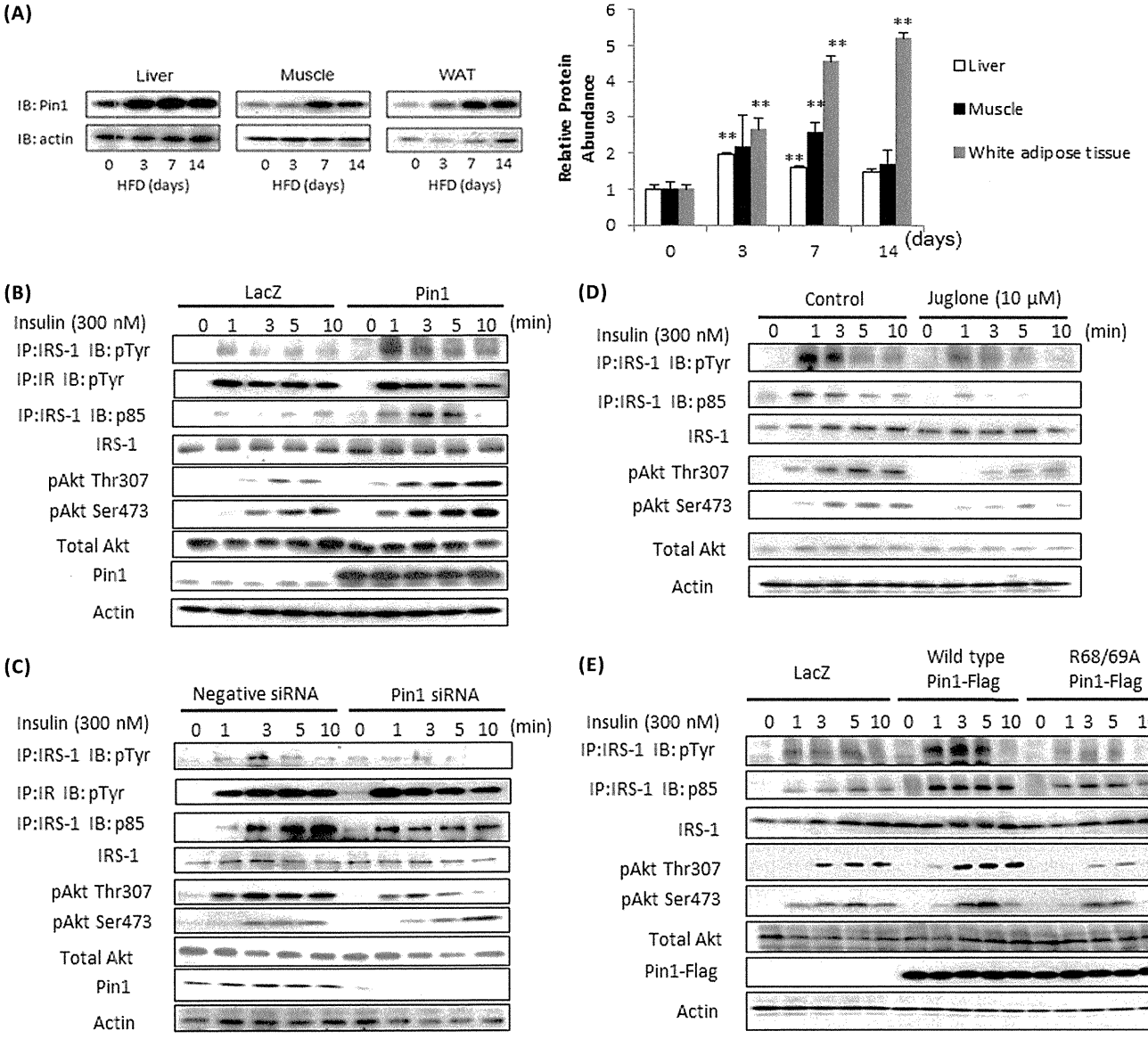

FIGURE 1. **Pin1 enhances insulin signaling.** *A*, mice were fed a control diet or HFD for the indicated periods. Liver, muscle, and adipose tissue lysates were prepared, then immunoblotted (*IB*) with anti-Pin1 or anti-actin antibody. *B* and *C*, Pin1 enhances insulin-induced IRS-1 phosphorylation and its downstream signaling. *B*, LacZ or Pin1 was overexpressed in HepG2 cells. *IP*, immunoprecipitates. *C*, HepG2 cells were treated with control siRNA or Pin1 siRNA. In both experiments, at the indicated times after initiating insulin stimulation, lysates were prepared from HepG2 cells. Then phosphorylation levels and protein amounts of IRS-1, p85 associated with IRS-1 and Akt Thr-307 and Ser-473 phosphorylations, and the Pin1 were determined. *D*, the Pin1 inhibitor Juglone attenuated the insulin-induced IRS-1 phosphorylation in HepG2 cells. HepG2 cells were treated with or without 10 μM Juglone for 30 min. At the indicated times after initiating insulin stimulation, lysates were prepared from HepG2 cells. Then phosphorylation levels and protein amounts of IRS-1, p85 associated with IRS-1, Akt Thr-307 and Ser-473 phosphorylations were determined. *E*, wild-type, but not the inactive mutant of Pin1, enhanced insulin-induced IRS-1 phosphorylation and its downstream signaling. LacZ, wild-type Pin1, or R68A/R69A-mutated Pin1 was overexpressed in HepG2 cells. At the indicated times after initiating insulin stimulation, lysates were prepared from HepG2 cells. Then, phosphorylation levels and protein amounts of IRS-1, p85 associated with IRS-1, and Akt Thr-307 and Ser-473 phosphorylations were determined. A representative immunoblot from four independent experiments is shown.

Transphor; Amersham Biosciences) and subjected to immunoblotting using the Super Signal West Pico Chemiluminescence System (Pierce). The results of several immunoblots were quantitatively analyzed using an LAS-3000 mini (FUJIFILM, Tokyo, Japan).

Supernatants containing equal amounts of protein (2 mg) were incubated with anti-IRS-1 and anti-IRS-2 antibodies (5 μg each) and then with 100 μl of protein A- and G-Sepharose. These immunoprecipitates and cell lysates were boiled in Laemmli sample buffer containing 100 mmol/liter dithiothreitol, electrophoresed, and immunoblotted with anti-IRS-1, anti-IRS-2, anti-p85 (phosphatidylinositol-3-kinase), anti-Pin1, phospho-Akt (Thr-308 and Ser-473), or 4G10 antibody. The bands were quantitatively analyzed using the LAS-3000 mini.

Preparation of Baculovirus-produced Recombinant Proteins—Full-length coding regions of human Pin1, GFP-tagged Pin1, IRS-1, and DsRed-tagged full-length and deletion mutants of IRS-1 were subcloned into pBacPAK9 transfer vector (Clontech, Mountain View, CA), and baculoviruses were prepared according to the manufacturer's instructions. For protein production, Sf9 cells were infected with these baculoviruses and grown for 48 h.

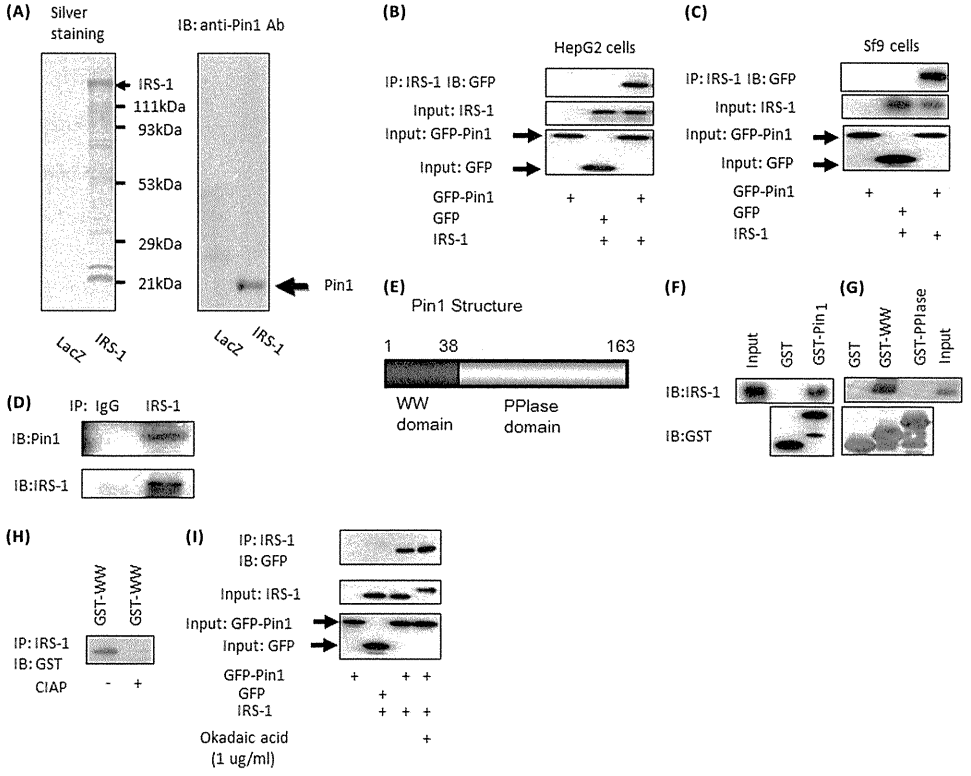

FIGURE 2. *A*, Pin1 association with IRS-1 is shown. IRS-1 with the N-terminal MEF tag was overexpressed in mouse liver using adenovirus gene transfer, and IRS-1-containing complexes were purified. The samples were electrophoresed, then silver-stained (*left panel*) and immunoblotted (*IB*) with anti-Pin1 antibody (*Ab, right panel*). *B*, IRS-1 or control LacZ was overexpressed with GFP or GFP-Pin1 in HepG2 cells. The cell lysates were immunoprecipitated (*IP*) with anti-IRS-1 antibody followed by immunoblotting with anti-GFP antibody. *C*, IRS-1 was overexpressed with GFP or GFP-Pin1 in Sf9 cells. The cell lysates were immunoprecipitated with anti-IRS-1 antibody followed by immunoblotting with anti-GFP antibody. *D*, the mouse liver cell lysates were immunoprecipitated with anti-IRS-1, and the immunoprecipitates were immunoblotted with anti-Pin1 and anti-IRS-1. *E*, Pin1 structure. GST-Pin1, GST-Pin1 WW domain, and GST-Pin1 PPIase domain were prepared. With incubation, these GST-proteins were conjugated to beads and cell lysates from IRS-1 overexpressing Sf-9 cells. *F*, GST-Pin1, but not GST alone, bound to IRS-1 *in vitro*. *G*, GST-WW, but not the GST-PPIase domain, bound IRS-1. *H*, lysates of Sf-9 cells overexprressing IRS-1 were treated with or without 40 units/ml alkaline phosphatase. Then the cell lysates were incubated with GST-WW domain and immunoprecipitated with anti-IRS-1 antibody. The immunoprecipitates were electrophoresed and immunoblotted with anti-GST antibody. *I*, HepG2 cells overexpressing IRS-1 or control LacZ were overexpressed with GFP or GFP-Pin1, then incubated with or without 1 μg/ml okadaic acid for 1 h. The cell lysates were immunoprecipitated with anti-IRS-1 antibody followed by immunoblotting with anti-GFP antibody.

Preparation of Glutathione S-transferase (GST)-Pin1 Fusion Protein—cDNAs encoding full-length human Pin1 and the WW and PPIase domains of Pin1 were subcloned into a pGEX-4T-1 vector (GE Healthcare), which was used to transform *Escherichia coli* JM105 (Promega, Madison, WI). Transformed cells were grown to an A_{600} of 0.6 in LB medium supplemented with 0.1 mg/ml ampicillin and stimulated for 3 h with 1.0 mM isopropyl-β-D-thiogalactopyranoside. GST fusion proteins were isolated and purified by affinity chromatography on a glutathione-Sepharose 4B column (GE Healthcare). Glutathione was removed by dialysis against phosphate-buffered saline containing 10 mM dithiothreitol.

RNA Interference—For the knockdown of human Pin1, a validated Stealth™ RNAi of human Pin1 (5′-CGGCAACAGCAGCAGUGGUGGCAAA-3′) was used. After RNAi and RNAiMAX in Opti-MEM had been mixed, they were introduced into HepG2. Forty-eight hours later, the cells were stimulated with insulin for the indicated times. Mouse Pin1 RNAi (5′-CACAGTATTTATTGTTCTAA-3′) was purchased from Invitrogen. Similarly, 48 h after introduction into 3T3-L1 cells, differentiation was induced by a mixture including isobutylmethylxanthine, dexamethasone, and insulin.

Intraperitoneal Glucose, Insulin, and Pyruvate Tolerance Tests—Mice were fasted for 14 h followed by blood sampling and intraperitoneal injection of glucose (2 g/kg body wt), insulin (0.75 units/kg body wt), or pyruvate (2 g/kg body wt). Whole venous blood was obtained from the tail vein at the indicated times after the glucose load. Blood glucose was measured with a portable blood glucose monitor.

In Vivo Insulin Stimulation—In brief, mice were anesthetized with pentobarbital sodium. The portal vein was exposed, and 0.4 ml of normal saline (0.9% NaCl) with or without insulin (25 milliunits/g of body wt) were injected. Livers were removed 30 s later, hind limb skeletal muscles 90 s thereafter, and immediately homogenized with a Polytron homogenizer in 6 volumes of solubilization buffer. Both extracts were centrifuged at 15,000 *g* for 30 min at 4 °C, and the supernatants were used as samples for immunoprecipitation and immunoblotting.

Glucose Uptake in Isolated Skeletal Muscle—Mice were anesthetized, and soleus muscles were dissected out and rapidly cut into 2–3-mg strips. Muscle strips were incubated in a shaking water bath at 35 °C for 60 min in a 20-ml flask containing 2.0 ml Krebs-Henseleit bicarbonate buffer supplemented with 8 mM glucose, 32 mM mannitol, and 0.1% bovine serum albumin

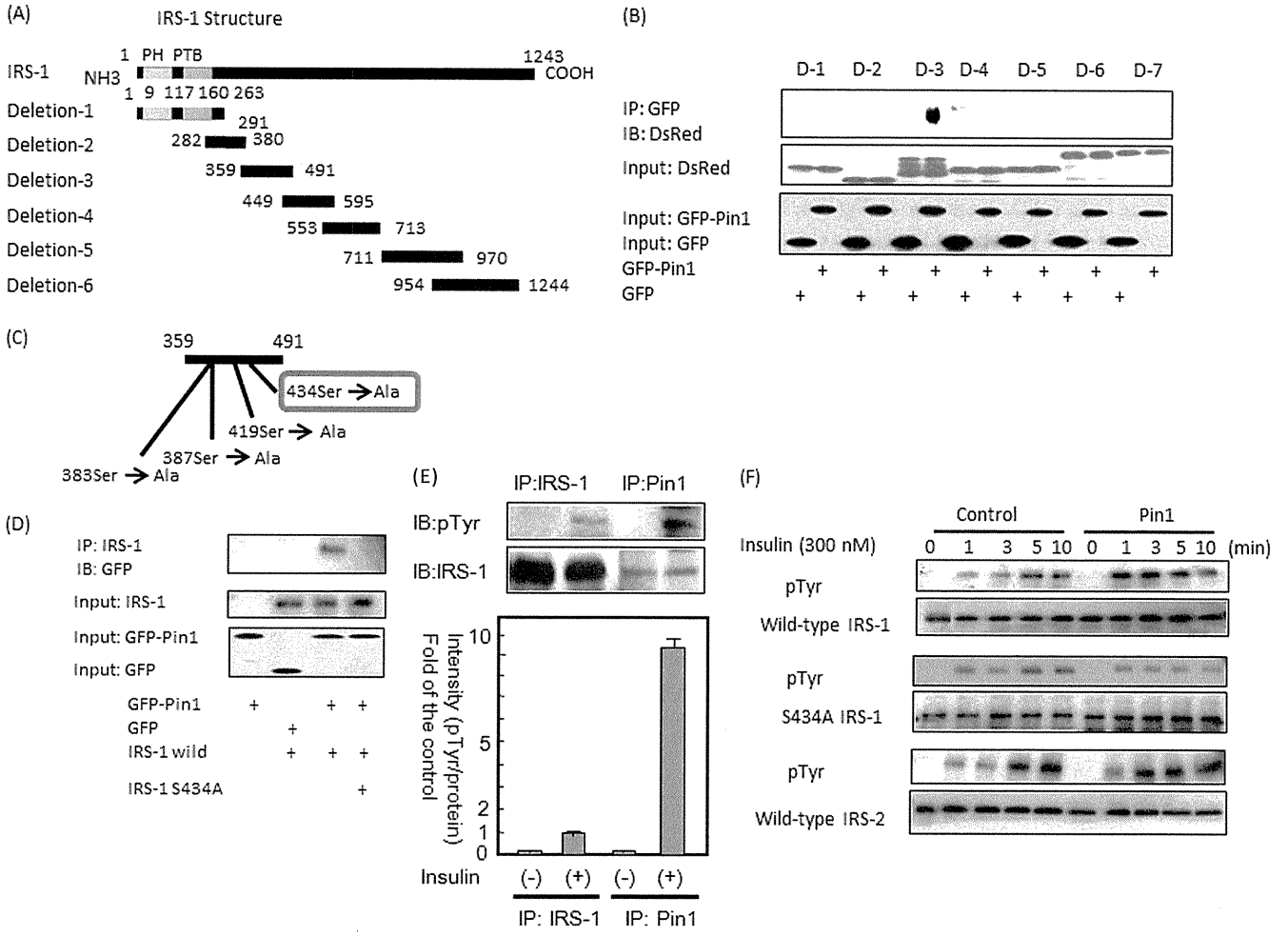

FIGURE 3. *A* and *B*, the constructs of IRS-1 deletion mutants are shown. Baculoviruses expressing these six mutants with the N-terminal DsRed tag were prepared. These six deletion mutants were overexpressed with GFP or GFP-Pin1 in Sf-9 cells. The cell lysates were immunoprecipitated (*IP*) with anti-GFP antibody followed by immunoblotting (*IB*) with anti-DsRed antibody. The *upper immunoblot* shows that mutant 3 binds to GFP-Pin1, but not to GFP alone. PH, pleckstrin homology; *PTB*, phosphotyrosine binding. *C* and *D*, shown are the orientations of four candidate Ser/Pro motifs in mutant 3 involved in the association with Pin1. Wild-type IRS-1 or IRS-1 S434A was overexpressed with GFP-Pin1 or GFP in Sf-9 cells. The cell lysates were immunoprecipitated with anti-IRS-1 antibody followed by immunoblotting with anti-GFP. The *upper panel* shows that, unlike the wild type, IRS-1 S434A does not associate with Pin1. *E*, HepG2 cells were stimulated with insulin for 3 min, then cell lysates were immunoprecipitated with anti-IRS-1 or anti-Pin1 antibody. Both samples were electrophoresed and immunoblotted with anti-Tyr(P) (*pTyr*) or anti-IRS-1 antibody (*upper panel*). The IRS-1 phosphorylation level and protein amount were calculated as the means ± S.E. of three samples (*, $p < 0.05$). *F*, MEF-tagged IRS-1, MEF-tagged S434A IRS-1, and MEF-tagged IRS-2 were overexpressed with control LacZ or Pin1 in HepG2 cells. Cell lysates were then immunoprecipitated with anti-FLAG-tag antibody and immunoblotted with anti-Tyr(P) and anti-FLAG-tag antibodies.

(BSA) (radioimmunoassay grade). Flasks were gassed continuously with 95% O_2, 5%CO_2 throughout the experiment. The muscles were then incubated for 20 min in oxygenated KRB buffer in the presence or absence of human insulin (2 milliunits/ml) and then incubated for 20 min at 29 °C in 1.5 ml of KRB buffer containing 8 mM 2-deoxy-D- [1,2-^{3}H(*N*)]glucose (2.25 μCi/ml), 32 mM [^{14}C]mannitol (0.3 μCi/ml), 2 mM sodium pyruvate, and 0.1% BSA. After the incubation, muscles were rapidly blotted, weighed, and solubilized with 1 ml of Soluene 350 (PerkinElmer Life Sciences). The samples were counted in a liquid scintillation counter. 2-Deoxy-[^{3}H]glucose uptake rates were corrected for extracellular trapping using [^{14}C]mannitol counts.

Quantitative Real-time Reverse Transcription-PCR—Total RNA was extracted from 3T3-L1 adipocytes or mouse liver and epididymal adipose tissue using Sepasol reagent (Nakalai Tesche, Kyoto, Japan). First-strand cDNAs were synthesized using PrimeScript reverse transcriptase with oligo(dT). Real-time PCR was performed using SYBR Green PCR master mix (Invitrogen) on an ABI Prism 7000 sequence detection system (Applied Biosystems, Foster City, CA). The primers were designed as follows: SREBP1 forward: GGAGCCATGGATTGCACATT; SREBP1 reverse, GGCCCGGGAAGTCACTGT; SREBP2 forward, TAACCCCTTGACTTCCTTGCT; SREBP2 reverse, TGCTCTTAGCCTCATCCTCAA; ACC forward, TCTCTGGCTTACAGGATGGTTTG; ACC reverse, GAGTCTATTTTCTTTCTGTCTCGACCTT; FAS forward, GCTGCGGAAACTTCAGGAAAT; FAS reverse, AGAGACGTGTCACTCCTGGACTT; SCD forward, GTCAAAGAGAAGGGCGGAAAAC; SCD reverse, AAGGTGTGGTGGTAGTTGTGGAAG.

Statistical Analysis—Results are expressed as the means ± S.E., and significance was assessed using one way analysis of variance unless otherwise indicated.

RESULTS

Increased Pin1 Expression in Mouse Liver, Muscle, and Fat Tissue with High-fat Diet Feeding—We previously reported that Pin1 protein is increased in the fed state (19). In this study we speculated that Pin1 expression might be regulated by altered nutrient conditions and examined Pin1 expression alteration in mice fed a HFD. As shown in Fig. 1*A*, HFD feeding markedly increased Pin1 protein in liver, muscle, and epididymal fat tissue. Pin1 amounts in other tissues such as the brain were not significantly altered (supplemental Fig. 1).

Enhancing Effect of Pin1 on Insulin Signaling—Because Pin1 expression was affected by nutrient conditions, we examined the possible involvement of Pin1 in glucose and lipid metabolism regulation. First, to elucidate the effect of Pin1 on insulin signaling, HA-tagged Pin1 was overexpressed in HepG2 cells (Fig. 1*B* and supplemental Fig. 2*A*). The overexpressed Pin1 amount was ~5-fold that of endogenous Pin1. In this state, insulin-induced IRS-1 phosphorylation and p85 association with IRS-1 and Akt phosphorylation were all markedly enhanced, whereas IRS-1 and Akt protein amounts were unchanged. Pin1 gene suppression using siRNA attenuated these events (Fig. 1*C* and supplemental Fig. 2*B*). Similar data were obtained using the Pin1-specific inhibitor Juglone, which has no effects on the activities of other prolyl isomerases, such as FKBP (FK506-binding protein) and cyclophilin A (21) (Fig. 1*D* and supplemental Fig. 2*C*). In addition, overexpression of the inactive mutant of Pin1 (R68A/R69A), in which Arg-68 and Arg-69 are replaced by Ala, failed to enhance insulin signaling (Fig. 1*E* and supplemental Fig. 2*D*). Thus, Pin1 expression level and activity regulate the efficiency of insulin-induced IRS-1 phosphorylation.

Association of Pin1 with IRS-1—Because Pin1 markedly enhanced insulin-induced IRS-1 phosphorylation, we considered a direct association of Pin1 with IRS-1. First, we used an MEF-tagged purification system, *i.e.* IRS-1 fused with N-terminal triple tags consisting of an myc tag, tobacco etch virus protease cleavage sequence, and FLAG tag overexpressed in mouse liver. Sequential affinity purification was performed using three steps; myc tag antibody immunoprecipitation, elution by tobacco etch virus protease digestion, and finally, FLAG tag antibody immunoprecipitation. Purified IRS-1 containing complexes were electrophoresed and then silver-stained, which demonstrated bait proteins of IRS-1 and many others including 14-3-3 proteins. Immunoblotting using Pin1 antibody indicated the presence of Pin1 in IRS-1 complexes (Fig. 2*A*). To confirm the association between IRS-1 and Pin1, IRS-1 and either GFP-Pin1 or GFP was co-overexpressed in HepG2 or Sf-9 cells. As shown in Fig. 2, *B* and *C*, GFP-Pin1, but not GFP alone, was detected in IRS-1 immunoprecipitates. Furthermore, Pin1 was detected in immunoprecipitates with anti-IRS-1 antibody, but not control IgG, from mouse liver (Fig. 2*D*). Thus, the association between IRS-1 and Pin1 is physiological.

To identify the Pin1 domain responsible for the association with IRS-1, GST-Pin1, the GST-Pin1 WW domain, and the GST-Pin1 PPIase domain were prepared (Fig. 2*E*). These GST proteins were conjugated to beads and incubated with cell lysates from IRS-1-overexpressing Sf-9 cells. GST-Pin1, but not

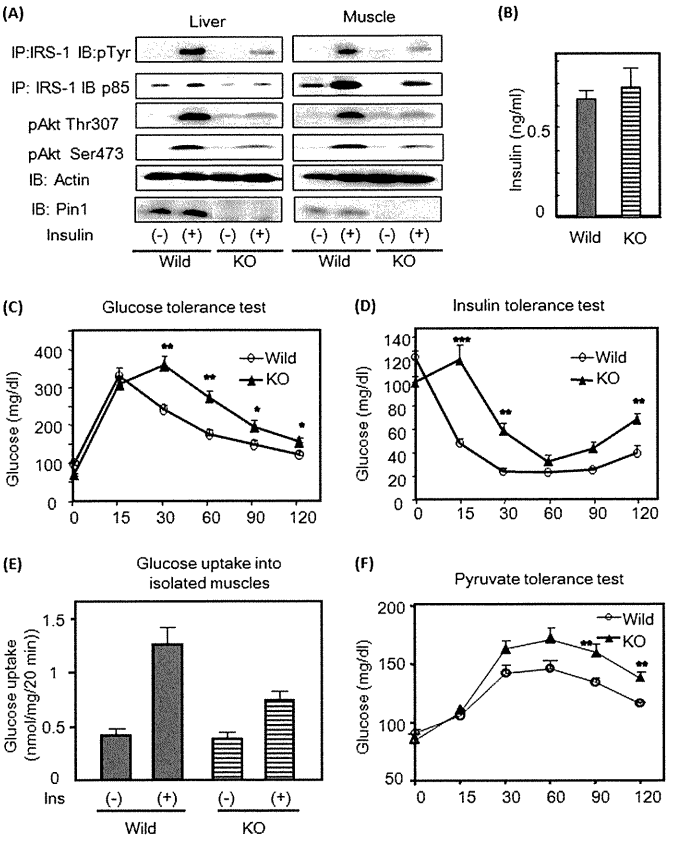

FIGURE 4. **Pin1 KO mice exhibit insulin resistance.** *A*, insulin was injected into control and Pin1 KO mice, and IRS-1 and Akt phosphorylations were determined. *IB*, immunoblot. *B*, fasting insulin concentrations in control and Pin1 KO mice are shown. *C*, glucose tolerance test results are shown. 2 mg/kg glucose was injected into control and Pin1 KO mice, and blood glucose concentrations were measured as indicated. *D*, insulin tolerance test results are shown. 0.75 units/kg insulin was injected intraperitoneally into control, and Pin1 KO mice and blood glucose concentrations were measured as indicated. *E*, shown is glucose uptake into isolated muscle. *F*, pyruvate tolerance test results are shown. 2 mg/kg pyruvate was injected into control, and Pin1 KO mice and blood glucose concentrations were measured, as indicated. The results are presented as the means (±S.E.) of six independent experiments (*, $p < 0.05$; **, $p < 0.01$).

GST alone, bound to IRS-1 *in vitro* (Fig. 2*F*). This pulldown system experiment revealed the GST-WW domain, but not that of GST-PPIase, to bind IRS-1 (Fig. 2*G*). In addition, treating IRS-1 with alkaline phosphatase completely abolished the association with Pin1 (Fig. 2*H*), whereas okadaic acid treatment significantly increased this association (Fig. 2*I*), suggesting involvement of serine and/or threonine phosphorylation in IRS-1.

Subsequently, six DsRed-tagged IRS-1 deletion (N termini) mutants (Fig. 3*A*) and GFP-tagged Pin1 were co-overexpressed in Sf-9 cells. As shown in Fig. 3*B*, the IRS-1 deletion mutant 3 containing amino acids 359–491 was immunoprecipitated with GFP-tagged Pin1. There are four serine-proline motifs in this portion (Fig. 3*C*). Each of these serine residues was replaced with alanine, and the mutant not associating with Pin1 was examined. As shown in Fig. 3*D*, IRS-1 with serine 434 replaced by alanine did not bind Pin1, indicating that the association between IRS-1 and Pin1 is mediated via the phosphoserine 434-containing motif in IRS-1 and the WW domain in Pin1. Ser-434 is in the SAIN (Shc and IRS-1 NPXY binding) domain, which

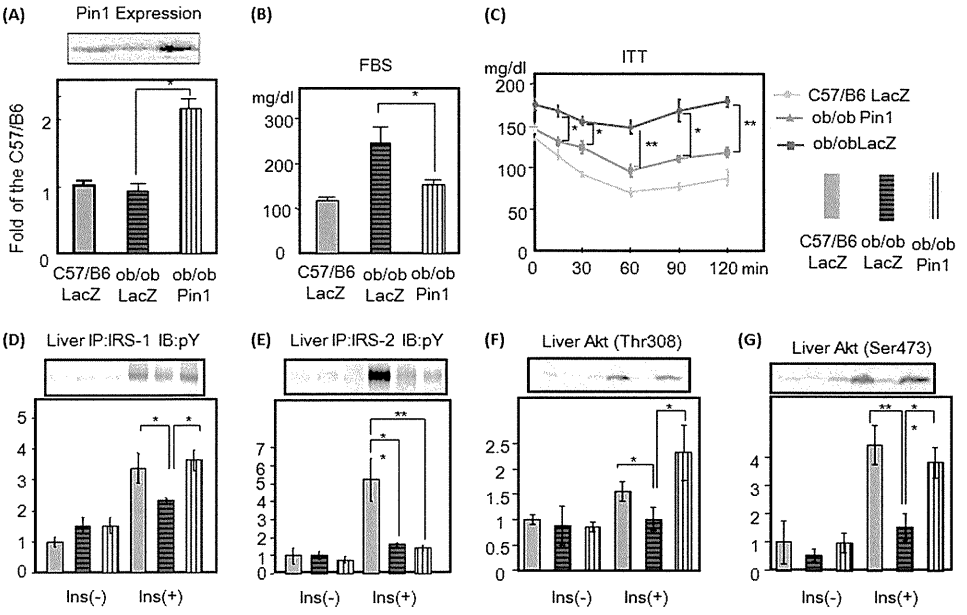

FIGURE 5. **Hepatic overexpression of Pin1 normalizes the hyperglycemia with insulin resistance in *ob/ob* mice.** LacZ or Pin1 adenovirus was injected via the tail vein. *A*, after 72 h, liver cell lysates were prepared, and the Pin1 expression level was determined by immunoblotting with anti-Pin1 antibody. The *upper panel* is a representative blot, and the *lower graph* shows the quantitative analysis ($n = 6$). *B*, shown are fasting blood glucose concentrations in C57/B6, *ob/ob* overexpressing LacZ, and *ob/ob* overexpressing Pin1 mice. *C*, insulin tolerance tests (*ITT*) for the three groups are shown. *D* and *E*, tyrosine phosphorylations of hepatic IRS-1 and IRS-2 are shown. Mice were injected with insulin via the portal vein, and phosphorylations of IRS-1 and IRS-2 were examined as reported previously. *IP*, immunoprecipitation; *pY*, Tyr(P). *F* and *G*, Akt phosphorylations at Thr-308 and Ser-473 were also examined in the livers of all three groups. $n = 6$ for each group and representative blots are shown in the *upper panels*. The results are presented as graphs with means (±S.E.). *, $p < 0.05$; **, $p < 0.05$.

has been suggested to be involved in the association with the activated insulin receptor (22, 23). IRS-1 contains many serine/threonine residues that are heavily phosphorylated even under basal conditions, and Ser-434 is probably one such residue.

Furthermore, to test whether or not enhanced IRS-1 phosphorylation is really mediated by direct association between IRS-1 and Pin1, insulin-induced phosphorylation levels of IRS-1 were compared between immunoprecipitation with IRS-1 antibody *versus* anti-Pin1 antibody using HepG2 cells. There was much less IRS-1 in the anti-Pin1 antibody immunoprecipitate than in the anti-IRS-1 immunoprecipitate, whereas insulin-induced IRS-1 phosphorylation was far greater with anti-Pin1 antibody immunoprecipitated IRS-1 (Fig. 3*E*). The tyrosine phosphorylation level/IRS-1 protein ratio was extremely high in the anti-Pin1 antibody immunoprecipitate as compared with the whole IRS-1 ratio. In addition, the effects of Pin1 on insulin-induced phosphorylations of S434A-mutated IRS-1 unable to associate with Pin1 as well as on IRS-2 were examined (Fig. 3*F*). FLAG-tagged wild-type, S434A IRS-1, or FLAG-tagged IRS-2 were co-overexpressed with Pin1 or LacZ in the HepG2 cells. The insulin-induced tyrosine phosphorylation of S434A IRS-1 was unaffected by Pin1 overexpression, whereas that of wild-type IRS-1 was markedly enhanced (Fig. 3*F*). It is noteworthy that IRS-2 phosphorylation is not significantly altered by Pin1. The phosphorylation of endogenous IRS-2 was also unaffected by Pin1 overexpression, although IRS-2 binds to Pin1 when overexpressed in HepG2 cells (supplemental Fig. 3). Our observations suggest that association of Pin1 with IRS-1 markedly enhances insulin-induced IRS-1 phosphorylation and its downstream signaling.

Insulin Resistance and Glucose Intolerance in Pin1 KO Mice—To elucidate the *in vivo* role of Pin1 in metabolism, the insulin signaling and sensitivity of Pin1 KO mice (20) were investigated. Insulin signaling was investigated first. Injecting insulin via the portal vein revealed insulin-induced IRS-1 tyrosine phosphorylation, the association of p85 with IRS-1 and Akt phosphorylation weaker in Pin1 KO liver and muscle than in those of wild-type mice (Fig. 4*A* and supplemental Fig. 4). Glucose and insulin tolerance tests demonstrated the insulin resistance of Pin1 KO mice (Fig. 4, *C* and *D*), whereas fasting serum insulin concentrations did not differ (Fig. 4*B*). The insulin-induced glucose uptake into isolated soleus muscle was also decreased in Pin1 KO mice as compared with controls, indicating muscle insulin resistance (Fig. 4*E*). The pyruvate tolerance test showed higher blood glucose concentrations in Pin1 KO mice, suggesting hepatic insulin resistance in these mice (Fig. 4*F*). Thus, in Pin1 KO mice, IRS-1 phosphorylation and downstream events are attenuated, and insulin resistance is present in both liver and muscle.

Hepatic Pin1 Overexpression Improves Insulin Resistance in ob/ob Mice—Interestingly, Pin1 expression was not altered in *ob/ob* mice as compared with lean controls. The reason is unclear, but we speculate that lack of a Pin1 expression response would exacerbate lipid and glucose metabolism abnormalities in *ob/ob* mice. We examined whether Pin1 overexpression might improve insulin resistance in *ob/ob* mice. Adenovirus for expressing Pin1 was injected intravenously. Adenovirus-mediated gene expression is reportedly limited to the liver (24) if adenovirus is injected into the bloodstream. Indeed, 72 h after injection, the amount of Pin1 was increased in the liver but not in muscle or adipose tissue (Fig. 5*A* and supplemental Fig. 5). In *ob/ob* mice, insulin-induced tyrosine phosphorylations of IRS-1 and IRS-2 and phosphatidylinositol 3-kinase/Akt activations were markedly impaired as

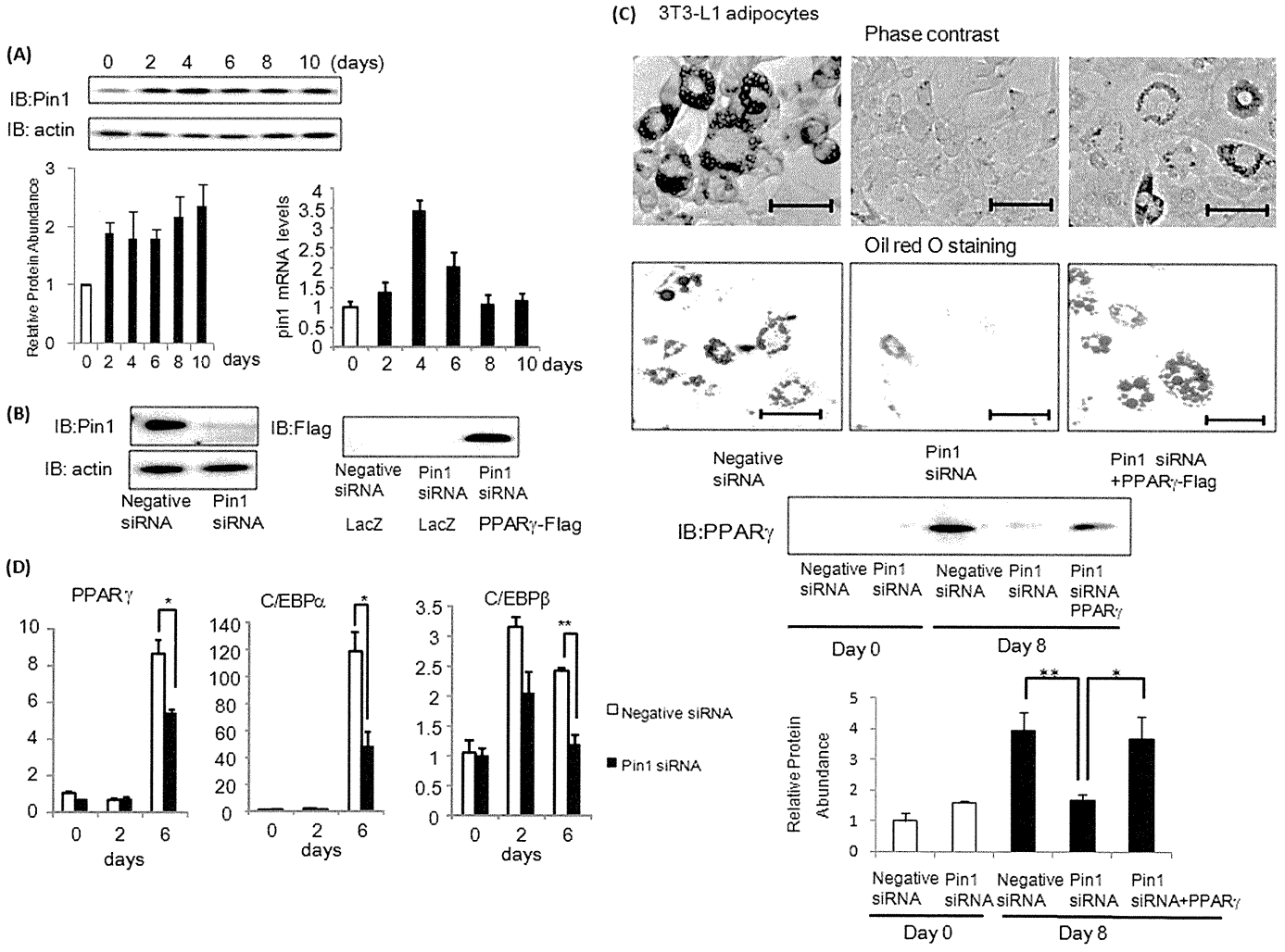

FIGURE 6. **Pin1 plays a critical role in adipose differentiation.** *A*, 3T3-L1 preadipocytes were induced to differentiate into adipocytes, and Pin1 protein and mRNA levels were determined at the indicated periods after initiation of differentiation. *IB*, immunoblots. *B*, 3T3-L1 preadipocytes were treated with Pin1 siRNA. The amounts of Pin1 and actin protein were determined with immunoblotting. *C*, 3T3-L1 preadipocytes were treated with control or Pin1 siRNA,or in combination with Pin1 siRNA and FLAG-tagged PPARγ adenovirus gene transfer. These cells were then induced to differentiate into adipocytes. Microscopic observations and oil red O staining results at 8 days are shown. Expression of PPARγ protein was detected as a marker of adipocyte maturity. *Scale bars* = 50 μm. *D*, before and 2 or 6 days after the induction of differentiation, PPARγ, c/EBPα, and c/EBPβ mRNA levels of 3T3-L1 cells were determined by real-time PCR. *, $p < 0.05$; **, $p < 0.05$.

reported previously (25) (Fig. 5, *D–G*). Pin1 overexpression normalized the decreased insulin-induced IRS-1, but not IRS-2, phosphorylation (Fig. 5, *D* and *E*). Hepatic Akt phosphorylations were also restored by Pin1 overexpression (Fig. 5, *F* and *G*). As reflected by improved insulin-signaling, glucose tolerance improved, *i.e.* fasting glucose concentrations (Fig. 5*B*) and expression levels of PEPCK and glucose-6-phosphatase were normalized (supplemental Fig. 6). The insulin tolerance test response was also improved (Fig. 5*C*). Thus, Pin1 overexpression improves insulin sensitivity in *ob/ob* mice.

Critical Role of Pin1 in Adipose Differentiation—Given the known role of insulin in adipose differentiation (26) and the increased Pin1 expression in WAT with HFD feeding, we speculated that Pin1 plays a critical role in diet-induced adipogenesis. First, Pin1 expression was shown to be up-regulated in 3T3-L1 cells during adipose differentiation (Fig. 6*A*). Then, the effect of Pin1 gene silencing using siRNA on adipose differentiation of 3T3-L1 adipocytes or human preadipocytes was examined (Fig. 6, *B* and *C*, and supplemental Fig. 7). Adipose differentiation of these cells was markedly impaired with suppressed inductions of PPARγ, c/EBPα, and C/EBPβ, known as master regulator genes of adipose differentiation (27–29) (Fig. 6*D*). In addition, expression of PPARγ protein, a marker of mature adipocytes, was reduced by Pin1 knockdown (Fig. 6*C*). Compensatory overexpression of PPARγ overcomes the suppressive effect of Pin1 siRNA on adipose differentiation (Fig. 6*C*).

Next, the adipose tissue of Pin1 KO mice was investigated. In normal mouse epididymal adipose tissue, PPARγ, c/EBPα, and CEBP/β as well as SREBP1, SREBP2, acetyl-CoA carboxylase, fatty acid synthase, and stearoyl-CoA-desaturase were markedly up-regulated by HFD feeding, which contributed to the enlargement of adipose tissues. In contrast, in Pin1 KO mouse adipose tissues, these increased gene expressions were significantly suppressed (Fig. 7, *A* and *B*), thereby markedly suppressing adipose tissue enlargement and weight gain on the HFD (Fig. 7, *C* and *D*). Thus, we concluded that Pin1 is a key regulator of diet-induced adipo-

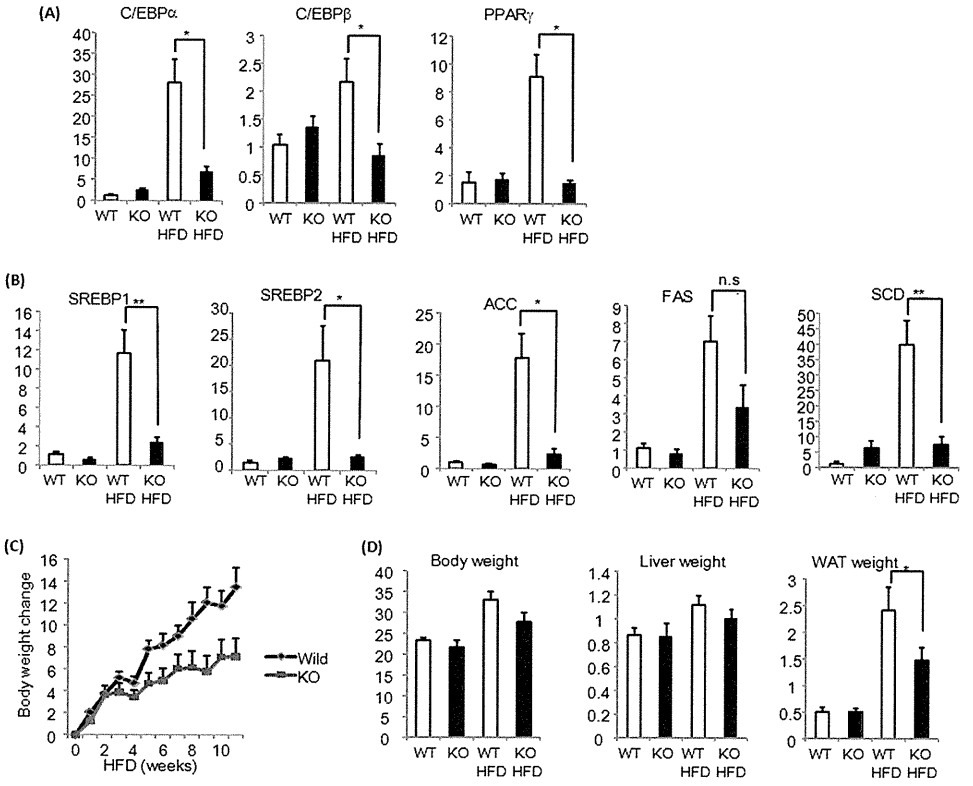

FIGURE 7. **Pin1 KO mice are resistant to HFD-induced obesity.** *A*, PPARγ, c/EBPα, and c/EBPβ mRNA levels in the adipose tissues of wild-type or Pin1 KO mice, fed a control diet or HFD for 4 weeks, were determined. *B*, SREBP1, SREBP2, ACC, FAS, and SCD mRNA levels in adipose tissues from wild-type or Pin1 KO mice, fed a control or HFD for 4 weeks, were determined by real-time PCR. *C*, weight gain after HFD feeding was compared between wild-type and Pin1 KO mice. *D*, the weights of the liver and adipose tissue were compared between wild-type and Pin1 KO mice, which had been fed either a control diet or HFD for 4 weeks. *ACC*, acetyl-CoA carboxylase; *FAS*, fatty acid synthase; *SCD*, stearoyl-CoA-desaturase.

genesis as Pin1 KO mice were clearly resistant to HFD-induced obesity.

DISCUSSION

Pin1 amounts increased according to nutrient state, as shown by marked elevation on a high-fat as compared with a normal diet. The Pin1 level was also higher in the fed than in the fasted state (19). Whereas previous studies have shown that Pin1 expression generally correlates with cell proliferative potential in normal tissues (7, 12) and is further up-regulated in many human cancers (30, 31), our findings are the first suggesting a relationship between Pin1 protein and nutrient conditions.

We also demonstrated that Pin1 is a positive regulator of insulin signaling via enhanced insulin-induced IRS-1 phosphorylation, based on a data series obtained using *in vitro* and *in vivo* overexpression of Pin1, gene silencing, a specific inhibitor, and Pin1 KO mice. The principal insulin receptor substrates, IRS-protein family members such as IRS-1 and IRS-2, adaptor proteins from the activated insulin receptor, are tyrosine-phosphorylated and thereby activate phosphatidylinositol 3-kinase/Akt. Pin1 binds to the Ser-434-containing motif of IRS-1, which is in the SAIN domain, via its WW domain. Because the SAIN domain reportedly plays an important role in the association with the insulin receptor (21, 22), it is speculated that Pin1 modifies the conformation of the SAIN domain and thereby enhances IRS-1 tyrosine phosphorylation by the insulin receptor. Similar enhanced phosphorylation of signal transduction protein via association with Pin1 has been reported for STAT3 (32).

Regarding the downstream signaling from the insulin receptor, the phosphatidylinositol 3-kinase/Akt pathway activation is essential for almost all insulin-induced glucose and lipid metabolism activities, *e.g.* glucose uptake, glycogen synthesis, suppression of glucose output, and triglyceride synthesis. Thus, in the muscles of Pin1 KO mice showing impaired Akt activation, glucose incorporation into muscle with insulin stimulation was decreased.

Insulin-induced phosphatidylinositol 3-kinase/Akt activations also play a role in adipogenesis (25, 33). It was shown that Pin1-deficient preadipocytes clearly fail to differentiate into adipocytes. This suppression was accompanied by insufficient inductions of PPARγ, c/EBPα, and c/EBPβ. On the other hand, overexpression of PPARγ reversed the Pin1 siRNA-induced suppression of adipose differentiation. Although the molecular mechanisms underlying insulin-induced induction of adipogenic genes has yet to be fully elucidated, previous reports have shown the essential action of SREBPs for adipogenesis to probably be via regulation of its downstream PPARγ (34, 35). Indeed, in adipose tissue from Pin1 KO mice, SREBPs and downstream gene expressions were decreased. These observations indicate that, as a consequence of impaired adipose differentiation, Pin1 KO mice are resistant to HFD-induced obesity.

Based on our data series, we can speculate as to the physiological significance of Pin1 with respect to metabolic regula-

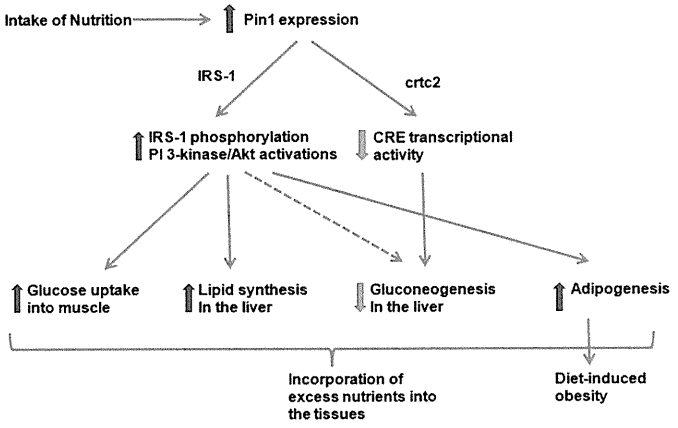

FIGURE 8. **Schema show the role of Pin1 in glucose and lipid metabolism in response to nutrient intakes.**

tion. When nutrients enter the body, excess glucose, lipids, and amino acids are stored mainly in the liver, muscle, and adipose tissue. Although insulin is the critical hormone for this process, we consider Pin1 to be involved in the mechanisms enhancing insulin sensitivity in peripheral tissues. Increased Pin1 expression functions to increase insulin sensitivity, thereby maintaining homeostasis in response to food or excess nutrient intake. Intriguingly, Pin1 enhances the signal from IRS-1 but not that from IRS-2. Although IRS-2 bound to Pin1 when both were overexpressed in HepG2 cells (supplemental Fig. 3), no association of endogenous IRS-2 and Pin1 was detected (data not shown). Thus, it is likely that IRS-2 associates with Pin1 far less efficiently than does IRS-1, which might account for the different effects of Pin1 on IRS-1 and IRS-2. Although several studies have revealed different roles for IRS-1 and IRS-2 (36, 37), we speculate that selective enhancement of IRS-1 signaling may contribute to greater hepatic lipid synthesis, as IRS-1 phosphorylation lasts much longer than that of IRS-2. Indeed, constitutive Akt overexpression induces marked lipid accumulation in the liver with blood glucose lowering (24). Thus, increased Pin1 expression is considered to be a physiologically beneficial response to excess nutrient intake.

However, excessive energy intake eventually causes fatty liver and obesity, which lead to the development of metabolic syndrome. In this condition, several kinases including mammalian target of rapamycin (mTOR), inhibitory κB kinase β, c-Jun N-terminal kinase, extracellular signal regulated kinase, and S6 kinase, induce the phosphorylations of serine 307, 302 and 612 of IRS-1, leading to reduced insulin-induced IRS-1 tyrosine phosphorylations and thereby contributing to insulin resistance (38–43). Thus, the efficiency of IRS-1 tyrosine phosphorylations appears to be up-regulated by increased Pin1 association and down-regulated by the aforementioned multiple serine phosphorylations. We speculate that both phenomena take place under conditions of energy excess, but when prolonged, the latter down-regulating mechanism becomes dominant.

In conclusion, we have demonstrated the important role of Pin1 as a positive modulator of insulin signaling as well as an inducer of obesity. Thus, Pin1 might be regarded as somewhat of a double-edged sword in that it increases insulin sensitivity but also promotes obesity (Fig. 8). However, suppression of Pin1 activity specifically in adipocytes might be a novel preventive treatment for obesity. Otherwise, if hepatic lipid accumulation is not severe, agents increasing Pin1 expression or enzymatic activity, *i.e.* targeting Pin1, may hold promise for treating Type 2 diabetes mellitus by improving hepatic insulin sensitivity.

REFERENCES

1. Fischer, G., Wittmann-Liebold, B., Lang, K., Kiefhaber, T., and Schmid, F. X. (1989) *Nature* **337,** 476–478
2. Liu, J., Farmer, J. D., Jr., Lane, W. S., Friedman, J., Weissman, I., and Schreiber, S. L. (1991) *Cell* **66,** 807–815
3. Choi, J., Chen, J., Schreiber, S. L., and Clardy, J. (1996) *Science* **273,** 239–242
4. Loewith, R., Jacinto, E., Wullschleger, S., Lorberg, A., Crespo, J. L., Bonenfant, D., Oppliger, W., Jenoe, P., and Hall, M. N. (2002) *Mol. Cell* **10,** 457–468
5. Schreiber, S. L. (1991) *Science* **251,** 283–287
6. Kunz, J., and Hall, M. N. (1993) *Trends Biochem. Sci.* **18,** 334–338
7. Lu, K. P., Hanes, S. D., and Hunter, T. (1996) *Nature* **380,** 544–547
8. Wulf, G., Finn, G., Suizu, F., and Lu, K. P. (2005) *Nat. Cell Biol.* **7,** 435–441
9. Lu, K. P., and Zhou, X. Z. (2007) *Nat. Rev. Mol. Cell Biol.* **8,** 904–916
10. Takahashi, K., Uchida, C., Shin, R. W., Shimazaki, K., and Uchida, T. (2008) *Cell. Mol. Life Sci.* **65,** 359–375
11. Zhou, X. Z., Kops, O., Werner, A., Lu, P. J., Shen, M., Stoller, G., Küllertz, G., Stark, M., Fischer, G., and Lu, K. P. (2000) *Mol. Cell* **6,** 873–883
12. Winkler, K. E., Swenson, K. I., Kornbluth, S., and Means, A. R. (2000) *Science* **287,** 1644–1647
13. Zacchi, P., Gostissa, M., Uchida, T., Salvagno, C., Avolio, F., Volinia, S., Ronai, Z., Blandino, G., Schneider, C., and Del Sal, G. (2002) *Nature* **419,** 853–857
14. Zheng, H., You, H., Zhou, X. Z., Murray, S. A., Uchida, T., Wulf, G., Gu, L., Tang, X., Lu, K. P., and Xiao, Z. X. (2002) *Nature* **419,** 849–853
15. Lu, P. J., Wulf, G., Zhou, X. Z., Davies, P., and Lu, K. P. (1999) *Nature* **399,** 784–788
16. Pastorino, L., Sun, A., Lu, P. J., Zhou, X. Z., Balastik, M., Finn, G., Wulf, G., Lim, J., Li, S. H., Li, X., Xia, W., Nicholson, L. K., and Lu, K. P. (2006) *Nature* **440,** 528–534
17. Liou, Y. C., Sun, A., Ryo, A., Zhou, X. Z., Yu, Z. X., Huang, H. K., Uchida, T., Bronson, R., Bing, G., Li, X., Hunter, T., and Lu, K. P. (2003) *Nature* **424,** 556–561
18. Nakatsu, Y., Sakoda, H., Kushiyama, A., Ono, H., Fujishiro, M., Horike, N., Yoneda, M., Ohno, H., Tsuchiya, Y., Kamata, H., Tahara, H., Isobe, T., Nishimura, F., Katagiri, H., Oka, Y., Fukushima, T., Takahashi, S., Kurihara, H., Uchida, T., and Asano, T. (2010) *J. Biol. Chem.* **285,** 33018–33027
19. Ichimura, T., Yamamura, H., Sasamoto, K., Tominaga, Y., Taoka, M., Kakiuchi, K., Shinkawa, T., Takahashi, N., Shimada, S., and Isobe, T. (2005) *J. Biol. Chem.* **280,** 13187–13194
20. Fujimori, F., Takahashi, K., Uchida, C., and Uchida, T. (1999) *Biochem. Biophys. Res. Commun.* **265,** 658–663
21. Hennig, L., Christner, C., Kipping, M., Schelbert, B., Rücknagel, K. P., Grabley, S., Küllertz, G., and Fischer, G. (1998) *Biochemistry* **37,** 5953–5960
22. Gustafson, T. A., He, W., Craparo, A., Schaub, CD., and O'Neill, T. J. (1995) *Mol. Cell. Biol.* **15,** 2500–2508
23. Yenush, L., Makati, K. J., Smith-Hall, J., Ishibashi, O., Myers, M. G., Jr., and White, M. F. (1996) *J. Biol. Chem.* **271,** 24300–24306
24. Ono, H., Shimano, H., Katagiri, H., Yahagi, N., Sakoda, H., Onishi, Y., Anai, M., Ogihara, T., Fujishiro, M., Viana, A. Y., Fukushima, Y., Abe, M., Shojima, N., Kikuchi, M., Yamada, N., Oka, Y., and Asano, T. (2003) *Diabetes* **52,** 2905–2913
25. Kerouz, N. J., Hörsch, D., Pons, S., and Kahn, C. R. (1997) *J. Clin. Invest.* **100,** 3164–3172
26. Nakae, J., Kitamura, T., Kitamura, Y., Biggs, W. H., 3rd, Arden, K. C., and Accili, D. (2003) *Dev. Cell* **4,** 119–129
27. Umek, R. M., Friedman, A. D., and McKnight, S. L. (1991) *Science* **251,** 288–292

28. Tanaka, T., Yoshida, N., Kishimoto, T., and Akira, S. (1997) *EMBO J.* **16,** 7432–7443
29. Spiegelman, B. M. (1998) *Diabetes* **47,** 507–514
30. Ryo, A., Nakamura, M., Wulf, G., Liou, Y. C., and Lu, K. P. (2001) *Nat. Cell Biol.* **3,** 793–801
31. Wulf, G. M., Ryo, A., Wulf, G. G., Lee, S. W., Niu, T., Petkova, V., and Lu, K. P. (2001) *EMBO J.* **20,** 3459–3472
32. Lufei, C., Koh, T. H., Uchida, T., and Cao, X. (2007) *Oncogene* **26,** 7656–7664
33. Rosen, E. D., and MacDougald, O. A. (2006) *Nat. Rev. Mol. Cell Biol.* **7,** 885–896
34. Tontonoz, P., Kim, J. B., Graves, R. A., and Spiegelman, B. M. (1993) *Mol. Cell. Biol.* **13,** 4753–4759
35. Jiang, L., Wang, Q., Yu, Y., Zhao, F., Huang, P., Zeng, R., Qi, R. Z., Li, W., and Liu, Y. (2009) *PLoS One* **4,** e6884
36. Withers, D. J., Gutierrez, J. S., Towery, H., Burks, D. J., Ren, J. M., Previs, S., Zhang, Y., Bernal, D., Pons, S., Shulman, G. I., Bonner-Weir, S., and White, M. F. (1998) *Nature* **391,** 900–904
37. Taniguchi, C. M., Emanuelli, B., and Kahn, C. R. (2006) *Nat. Rev. Mol. Cell Biol.* **7,** 85–96
38. Hotamisligil, G. S., Peraldi, P., Budavari, A., Ellis, R., White, M. F., and Spiegelman, B. M. (1996) *Science* **271,** 665–668
39. Hirosumi, J., Tuncman, G., Chang, L., Görgün, C. Z., Uysal, K. T., Maeda, K., Karin, M., and Hotamisligil, G. S. (2002) *Nature* **420,** 333–336
40. Pirola, L., Johnston, A. M., and Van Obberghen, E. (2004) *Diabetologia* **47,** 170–184
41. Werner, E. D., Lee, J., Hansen, L., Yuan, M., and Shoelson, S. E. (2004) *J. Biol. Chem.* **279,** 35298–35305
42. Ozcan, U., Yilmaz, E., Ozcan, L., Furuhashi, M., Vaillancourt, E., Smith, R. O., Görgün, C. Z., and Hotamisligil, G. S. (2006) *Science* **313,** 1137–1140
43. Morino, K., Neschen, S., Bilz, S., Sono, S., Tsirigotis, D., Reznick, R. M., Moore, I., Nagai, Y., Samuel, V., Sebastian, D., White, M., Philbrick, W., and Shulman, G. I. (2008) *Diabetes* **57,** 2644–2651

Increased Systemic Glucose Tolerance with Increased Muscle Glucose Uptake in Transgenic Mice Overexpressing RXRγ in Skeletal Muscle

Satoshi Sugita[1], Yasutomi Kamei[1]*, Fumiko Akaike[1,2], Takayoshi Suganami[1], Sayaka Kanai[1], Maki Hattori[1,2], Yasuko Manabe[3], Nobuharu Fujii[3], Takako Takai-Igarashi[4], Miki Tadaishi[5,6], Jun-Ichiro Oka[2], Hiroyuki Aburatani[7], Tetsuya Yamada[8], Hideki Katagiri[8], Saori Kakehi[9], Yoshifumi Tamura[9,10], Hideo Kubo[11], Kenichi Nishida[11], Shinji Miura[5], Osamu Ezaki[5], Yoshihiro Ogawa[1,12]

1 Department of Molecular Medicine and Metabolism, Medical Research Institute, Tokyo Medical and Dental University, Tokyo, Japan, **2** Laboratory of Pharmacology, Faculty of Pharmaceutical Sciences, Tokyo University of Science, Chiba, Japan, **3** Graduate School of Human Health Sciences, Tokyo Metropolitan University, Tokyo, Japan, **4** Department of Bioinformatics, Graduate School of Biomedical Science, Tokyo Medical and Dental University, Tokyo, Japan, **5** Nutritional Science Program, National Institute of Health and Nutrition, Tokyo, Japan, **6** Department of Nutritional Science, Faculty of Applied Bioscience, Tokyo University of Agriculture, Tokyo, Japan, **7** Research Center for Advanced Science and Technology, University of Tokyo, Tokyo, Japan, **8** Department of Metabolic Diseases, Center for Metabolic Diseases, Tohoku University Graduate School of Medicine, Miyagi, Japan, **9** Department of Medicine, Metabolism and Endocrinology, School of Medicine, Juntendo University, Tokyo, Japan, **10** Sportology Center, Juntendo University, Tokyo, Japan, **11** Daiichi-Sankyo Co., Ltd., Tokyo, Japan, **12** Global Center of Excellence Program, International Research Center for Molecular Science in Tooth and Bone Diseases, Medical Research Institute, Tokyo Medical and Dental University, Tokyo, Japan

Abstract

Background: Retinoid X receptor (RXR) γ is a nuclear receptor-type transcription factor expressed mostly in skeletal muscle, and regulated by nutritional conditions. Previously, we established transgenic mice overexpressing RXRγ in skeletal muscle (RXRγ mice), which showed lower blood glucose than the control mice. Here we investigated their glucose metabolism.

Methodology/Principal Findings: RXRγ mice were subjected to glucose and insulin tolerance tests, and glucose transporter expression levels, hyperinsulinemic-euglycemic clamp and glucose uptake were analyzed. Microarray and bioinformatics analyses were done. The glucose tolerance test revealed higher glucose disposal in RXRγ mice than in control mice, but insulin tolerance test revealed no difference in the insulin-induced hypoglycemic response. In the hyperinsulinemic-euglycemic clamp study, the basal glucose disposal rate was higher in RXRγ mice than in control mice, indicating an insulin-independent increase in glucose uptake. There was no difference in the rate of glucose infusion needed to maintain euglycemia (glucose infusion rate) between the RXRγ and control mice, which is consistent with the result of the insulin tolerance test. Skeletal muscle from RXRγ mice showed increased Glut1 expression, with increased glucose uptake, in an insulin-independent manner. Moreover, we performed *in vivo* luciferase reporter analysis using *Glut1* promoter (*Glut1*-Luc). Combination of RXRγ and PPARδ resulted in an increase in *Glut1*-Luc activity in skeletal muscle *in vivo*. Microarray data showed that RXRγ overexpression increased a diverse set of genes, including glucose metabolism genes, whose promoter contained putative PPAR-binding motifs.

Conclusions/Significance: Systemic glucose metabolism was increased in transgenic mice overexpressing RXRγ. The enhanced glucose tolerance in RXRγ mice may be mediated at least in part by increased Glut1 in skeletal muscle. These results show the importance of skeletal muscle gene regulation in systemic glucose metabolism. Increasing RXRγ expression may be a novel therapeutic strategy against type 2 diabetes.

Citation: Sugita S, Kamei Y, Akaike F, Suganami T, Kanai S, et al. (2011) Increased Systemic Glucose Tolerance with Increased Muscle Glucose Uptake in Transgenic Mice Overexpressing RXRγ in Skeletal Muscle. PLoS ONE 6(5): e20467. doi:10.1371/journal.pone.0020467

Editor: Massimo Federici, University of Tor Vergata, Italy

Received March 15, 2011; **Accepted** April 26, 2011; **Published** May 31, 2011

Funding: This work was supported in part by a Grant-in-Aid for scientific research KAKENHI from the Japanese Ministry of Education, Culture, Sports, Science and Technology (MEXT, Tokyo, Japan), research grants from the Japanese Ministry of Health, Labor and Welfare, and by the joint research program of the Institute for Molecular and Cellular Regulation, Gunma University. S. Sugita is a Research Fellow of the Japan Society for the Promotion of Science. The funders had no role in study design, data collection and analysis, decision to publish, or preparation of the manuscript.

Competing Interests: HK and KN are currently employed by the commercial company Daiichi-Sankyo Co., Ltd. HK and KN were non-commercially involved in this study. This does not alter the authors' adherence to all the PLoS ONE policies on sharing data and materials. Therefore, HK and KN do not have competing interests to disclose.

* E-mail: kamei.mmm@mri.tmd.ac.jp

Introduction

The skeletal muscle, known as the largest organ in the human body, plays an important role in exercise, energy expenditure, and glucose metabolism. It is a major site of glucose disposal [1,2]. In type 2 diabetic subjects, glucose uptake in the skeletal muscle is impaired [2]. Blood glucose is taken up by the skeletal muscle via insulin-dependent and independent glucose transporters (Glut4

and Glut1, respectively) [3], where it is converted into glycogen. Increasing capacity of glucose uptake in the skeletal muscle is considered beneficial for the prevention and treatment of type 2 diabetes [3,4]. On the other hand, glucose metabolism in the skeletal muscle may affect the whole body metabolism; the skeletal muscle-specific inactivation of *Glut4* has resulted in defect in insulin action in the adipose tissue (glucose uptake) and liver (suppression of gluconeogenesis) [5]. Thus, identification of the molecular mechanisms involved in skeletal muscle glucose metabolism should help clarify the pathophysiology of diabetes.

Nuclear receptors are part of a large superfamily of transcription factors that includes receptors for steroids, retinoic acid, and thyroid hormones [6]. RXRs are heterodimeric partners of many nuclear receptors, such as retinoic acid receptors (RARs), thyroid hormone receptors (T3Rs), liver X receptors (LXRs), peroxisome proliferator activated receptors (PPARs), and RXRs themselves [6]. Among RXR heterodimer partners, activation of PPARδ in the skeletal muscle increases insulin sensitivity [7]. The RXR subfamily consists of RXRα, RXRβ, and RXRγ [6,8]. Although RXRγ is preferentially expressed in the skeletal muscle, its functional role is poorly understood. We have recently found that expression of retinoid X receptor γ (RXRγ) is changed in the skeletal muscle under nutritional conditions; RXRγ mRNA expression is down-regulated by fasting and recovered by refeeding [9]. In an attempt to explore the role of RXRγ in the skeletal muscle, we established transgenic mice overexpressing RXRγ in the skeletal muscle (RXRγ mice) and found that they exhibit increased triglyceride contents in the skeletal muscle as a result of increased expression of sterol regulatory element binding protein 1c (SREBP1c), a transcriptional master regulator of lipogenesis [9]. Indeed, RXRγ has been shown to enhance SREBP1c gene expression in C2C12 myocytes *in vitro* at least in part by heterodimerization with LXR [9]. On the other hand, we also found that blood glucose levels are lower in RXRγ mice than in control mice [9]. These observations, taken together, suggest that RXRγ plays a critical role in glucose and lipid metabolism in the skeletal muscle. However, the molecular mechanism involved in RXRγ regulation of glucose metabolism in the skeletal muscle and how it affects systemic glucose metabolism are poorly understood.

Here, we demonstrate enhanced glucose metabolism with increased Glut1 expression and glucose uptake in RXRγ mice. This study suggests that activation of the skeletal muscle RXRγ is a novel therapeutic strategy to treat or prevent type 2 diabetes.

Methods

Animals

C57BL6 mice were purchased from Charles River Japan (Yokohama, Japan). Generation of RXRγ mice under the control of the human α-actin promoter was described previously [9]. They were allowed free access to food (CRF-1; Charles River) and water, unless otherwise stated. All animal experiments were approved by Institutional Animal Care and Use Committee of Tokyo Medical and Dental University (approval ID: No. 0090041).

Blood analysis

Serum samples were obtained from mice, when fed *ad libitum*. Serum glucose levels were measured by the blood glucose test meter (Glutest PRO R; Sanwa-Kagaku, Nagoya, Japan). Serum concentrations of insulin were determined by the enzyme-linked immunosorbent assay (ELISA) kits (Morinaga Institute of Biological Science, Inc., Yokohama, Japan).

Glucose and insulin tolerance tests

For glucose tolerance test, D-glucose (1 mg/g of body weight, 10% (w/v) glucose solution) was administered by intraperitoneal injection after an overnight fast. For insulin tolerance test, human insulin (Humulin R; Eli Lilly Japan K.K., Kobe, Japan) was injected intraperitoneally (0.75 mU/g of body weight), when fed *ad libitum*.

Hyperinsulinemic-euglycemic clamp studies

We analyzed as described previously [10–12] with slight modification. Two days before the clamp studies, a catheter was inserted into the right jugular vein for infusion under general anesthesia with sodium pentobarbital. Studies were performed on mice under conscious and unstressed conditions after a 4-h fast. The clamp study began with a prime (4 mg/kg for 5 min) of [6,6-^{2}H] glucose (Cambridge Isotope Laboratories, Inc, Andover, MA) followed by continuous infusion at a rate of 0.5 mg/kg per minute for 2 hr to assess the basal glucose turnover. After the basal period, hyperinsulinemic-euglycemic clamp was conducted for 120 min with a primed/continuous infusion of human insulin (25 mU/kg prime for 5 min, 5 mU/kg/min infusion) and variable infusion of 20% glucose to maintain euglycemia (approximately 100 mg/dl). The 20% glucose was enriched with [6,6-^{2}H] glucose to approximately 2.5% as previously described [12]. To determine the enrichment of [6,6-^{2}H]glucose in plasma at basal and insulin stimulated state, samples were deproteinized with trichloroacetic acid and derivatized with *p*-aminobenzoic acid ethyl ester. The atom percentage enrichment of glucose$_{m+2}$ was then measured by high-performance liquid chromatography with LTQ-XL-Orbitrap mass spectrometer (Thermo Scientific, CA). The glucose$_{m+2}$ enrichment was determined from the m/z ratio 332.2: 330.2. The hepatic glucose production was calculated by using the rate of infusion of [6,6-^{2}H]glucose over the atom percent excess in the plasma minus the rate of glucose being infused. The insulin-stimulated whole-body glucose uptake was calculated by adding the total glucose infusion rate plus the hepatic glucose production [12].

Quantitative real-time PCR. Quantitative real-time PCR was performed as described [9]. Total RNA was prepared using Sepazol (Nacalai Tesque, Kyoto, Japan). cDNA was synthesized from 5 μg of total RNA using Superscript II reverse transcriptase (Invitrogen Inc., Carlsbad, CA) with random primers. Gene expression levels were measured with an ABI PRISM 7700 using SYBR Green PCR Core Reagents (Applied Biosystems, Tokyo, Japan). The primers used were as follows, RXRγ: Fw: 5′-CAC-

Table 1. Body and dissected tissue weight and blood glucose level in RXRγ mice (4-3 line).

	Wild-type	RXRγ
Body weight (g)	26.4±0.3	26.5±0.4
Epididymal fat mass (g)	0.138±0.004	0.156±0.090
Gastrocnemius muscle weight (g)	0.282±0.004	0.238±0.008**
Liver weight (g)	1.290±0.029	1.321±0.033
Glucose (mg/dL) basal	170.0±9.4	145.6±4.9*
Glucose (mg/dL) fasting	74.4±1.7	67.0±0.6**

Mice were males 12 weeks of age. The number of animals used was 6 for both wild-type control and RXRγ mice.
* $P<0.05$;
** $P<0.01$, compared with wild-type control.
Values are the means ± SE. These samples were also used in Fig 2*A, B,* and *D*.
doi:10.1371/journal.pone.0020467.t001

Table 2. Body and dissected tissue weight and blood glucose level in RXRγ mice (5-3 line).

	Wild-type	RXRγ
Body weight (g)	36.0±1.8	31.9±1.2
Epididymal fat mass (g)	1.030±0.191	0.861±0.134
Gastrocnemius muscle weight (g)	0.305±0.016	0.214±0.020**
Liver weight (g)	1.375±0.119	1.320±0.066
Glucose (mg/dL) basal	142.5±8.6	117.3±8.2
Glucose (mg/dL) fasting	67.2±1.6	53.3±2.5**

Mice were males 38 weeks of age. The number of animals used was 6 for both wild-type control and RXRγ mice.
** $P<0.01$, compared with wild-type control.
Values are the means ± SE.
doi:10.1371/journal.pone.0020467.t002

CCTGGAGGCCTATACCA-3′, Rv: 5′-AAACCTGCCTGGCTGTTCC-3′, Glut1: Fw: 5′-CCAGC TGGGA ATCGT CGTT-3′, Rv: 5′-CAAGT CTGCA TTGCC CATGAT-3′, Glut4: Fw: 5′-TCTGTGGGTGGCATGATCTCT-3′, Rv: 5′-GCCCTTTTCCTTCCCAACC-3′, glucose phosphate isomerase 1: Fw: 5′-AGCGCTTCAACAACTTCAGCT-3′, Rv: 5′-CAGAATATGCCCATGGTTGGT-3′, phosphoglycerate mutase 1: Fw: 5′-TCCTGAAACATCTGGAAGGTATCTC-3′, Rv: 5′-CAGTGGGCAGAGTGATGTTGAT-3′, fructose bisphosphatase 2: Fw: 5′-TGAATGCAATCCTGTGGCC-3′, Rv: 5′-TGGTTGCCATACCTCCTGCT-3′, pyruvate dehydrogenase kinase isoenzyme 1: Fw: 5′-GGACTTCTATGCGCGCTTCT-3′, Rv: 5′-CTGACCCGAAGTCCAGGAAC-3′, glycogen synthase 2: Fw: 5′-AGGATCATTCAGAGGAACCGC-3′, Rv: 5′-CCAGTCCAGGAGATCTGAGAGC-3′.

Tissue sampling for analysis of Glut1 and Glut4 protein levels

Skeletal muscles were homogenized in ice-cold buffer containing 250 mmol/L sucrose, 20 mmol/L 2-[4-(2-hydroxyethyl)-1-piperadinyl] ethonsulforic acid (HEPES) (pH 7.4), and 1 mmol/L EDTA, and centrifuged at 1200 g for 5 minutes. The supernatant was centrifuged at 200 000 g for 60 minutes at 4°C [13]. The resulting pellet was solubilized in Laemmli sample buffer containing dithiothreitol. Samples were subjected to Western blotting as described [14]. Antibodies used were those against Glut1 (#07-1401, Millipore, Temecula, CA), and Glut4 (SC-1606, Santa Cruz Biotechnology Inc., Santa Cruz, CA).

Muscle incubation and glucose transport

Glucose transport was measured as described [15]. Mice were fasted overnight and killed. The extensor digitorum longus (EDL) muscles were rapidly removed, each of which was mounted on the incubation apparatus and preincubated in Krebs-Ringer bicarbonate (KRB) buffer containing 2 mmol/l pyruvate for 30 min. The muscles were then incubated in KRB buffer in the absence or presence of 50 mU/ml insulin for 10 min. The buffers were kept at 37°C throughout the experiment and gassed continuously with 95% O_2 and 5% CO_2. Immediately after incubation, the muscle was transferred to KRB buffer containing 1 mmol/l 2-[^{3}H]-deoxy-d-glucose (1.5 μCi/ml) and 7 mmol/l d-[^{14}C]-mannitol (0.3 μCi/ml).

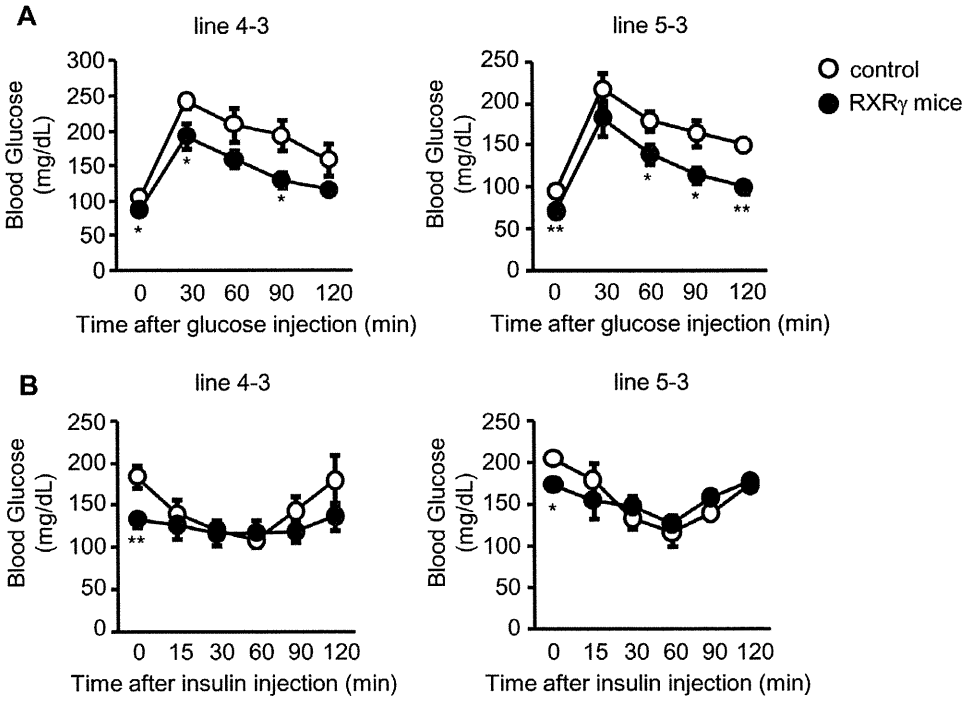

Figure 1. Glucose tolerance and insulin tolerance tests on RXRγ mice. (*A, B*) In A and B, male mice, 5 months of age, were used. The number of animals used was 6 for both control (open circles) and RXRγ (filled circles) mice of line 4-3, and 5 for both control (open circles) and RXRγ (filled circles) mice of line 5-3. * $P<0.05$ and ** $P<0.01$ compared with respective control.
doi:10.1371/journal.pone.0020467.g001

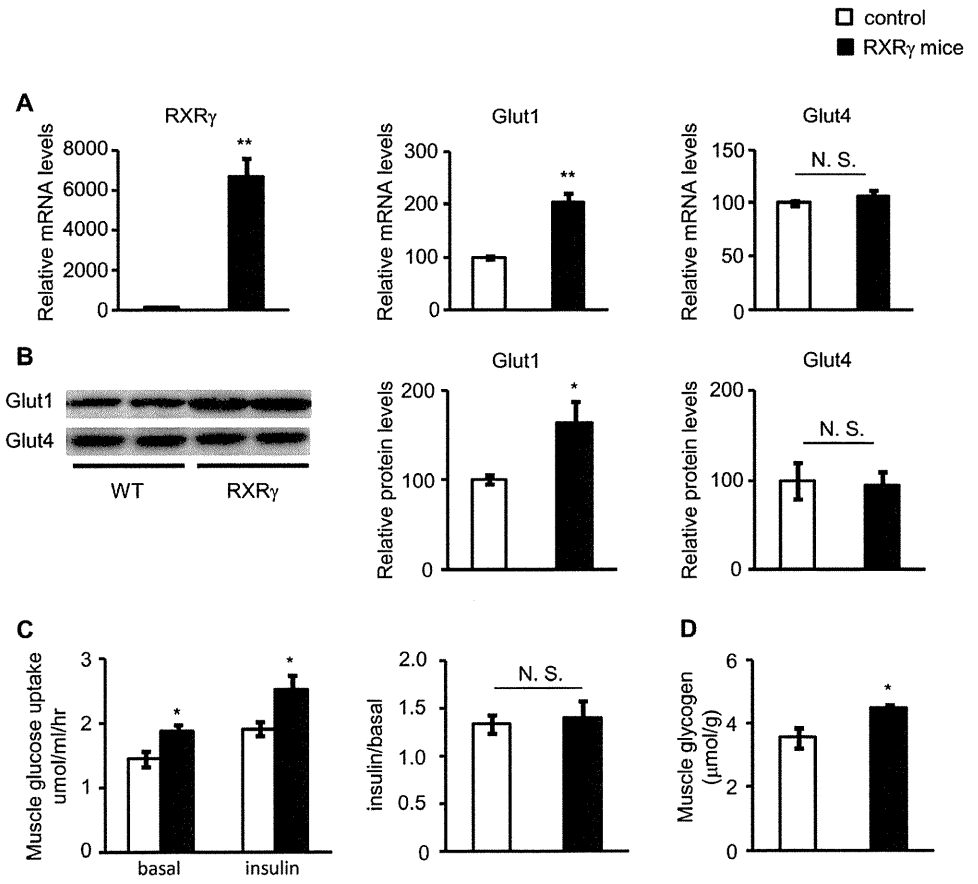

Figure 2. Levels of Glut 1 and Glut4, and glucose uptake in the skeletal muscle of RXRγ mice. (*A*) Gene expressions of *RXRγ*, *Glut1*, and *4* were examined by quantitative real-time PCR. The value for wild-type (littermates of line 4-3) mice was set at 100, and relative values are shown. (*B*) Protein levels of Glut1 and Glut4 were examined by Western blotting. Results of relative densitometric signal for Glut1 and 4 are shown. (*C*) Glucose uptake in the absence or presence of insulin and (*D*) glycogen content were increased in the skeletal muscle of RXRγ mice. Ratio of enhanced glucose uptake in the presence of insulin (insulin/basal) was similar in control and RXRγ mice. In *A*, *B* and *D*, the same samples were used. Mice were males of 12 weeks of age. The number of animals was 6 for both control (open bars) and RXRγ (filled bars) mice. These samples were also used in Table 1. In *C*, mice were males of 24–27 weeks of age. The number of animals was 6 for both control (open bars) and RXRγ (filled bars) mice. * $P<0.05$ and ** $P<0.01$ compared with respective control. N. S., not significant.
doi:10.1371/journal.pone.0020467.g002

Measurement of skeletal muscle glycogen

The skeletal muscle glycogen content was measured as glycosyl units after acid hydrolysis [16]. The skeletal muscle samples were minced, 50 mg of which was added to 1 ml of 0.3 M percholic acid and homogenized on ice. One ml of 1 N HCl was added and incubated for 2 h at 100°C, thereafter, 1 ml of 1 N NaOH was added at room temperature. Glucose content was examined using the F-kit glucose (Roche Diagnostics, Mannheim, Germany).

Plasmids

The coding region of mouse RXRγ and PPARδ cDNA were subcloned into a mammalian expression plasmid, pCMX [9]. The 1.5-kb 5′-flanking region of the mouse *Glut1* promoter was obtained by PCR with mouse genomic DNA (RefSeqs number: NC_000070). The PCR primers used were: Fw: 5′-GTGGTG-CGCGCCTGTAGTCC-3′ and Rv: 5′-GGCGCACTCCACG-GATGCCG-3′. The fragment was subcloned into the pGL3-basic luciferase vector (Promega Corporation, Madison, WI). The promoter regions used were: -1500 to +75, -647 to +75, and -152 to +75, counting the transcription start site as +1.

Electroporation and *in vivo* luciferase reporter analysis

In vivo electroporation was performed according to the modified method of Aihara and Miyazaki [17]. Under the pentobarbital anesthesia (30 mg/kg), bilateral quadriceps muscles from C57BL6

Table 3. Body weight, blood glucose and plasma insulin levels in RXRγ mice in clamp study.

		Wild-type	RXRγ
	Body weight (g)	24.1±1.2	23.4±0.3
Basal period	Glucose (mg/dL)	141.8±15.3	106.6±5.5*
	Insulin (ng/mL)	0.55±0.08	0.44±0.07
Clamp period	Glucose (mg/dL)	92.5±3.8	96.7±3.6
	Insulin (ng/mL)	2.60±0.20	2.38±0.33

Mice were males 13–16 weeks of age. The number of animals used was 6 for wild-type control mice and 7 for RXRγ mice.
* $P<0.05$, compared with wild-type control.
Values are the means ± SE. These mice were also used in Fig 3.
doi:10.1371/journal.pone.0020467.t003

mice (male, 12 weeks of age) were injected with 80 μg of plasmid DNA (25 μl) by using a 29-gauge needle attached to a 0.5-ml insulin syringe (Terumo Corporation, Tokyo, Japan). Square-wave electrical pulses (160 V/cm) were applied six times with an electrical pulse generator (CUY21EDIT, Nepa Gene Co. Ltd., Chiba, Japan) at a rate of one pulse per second, with each pulse being 20 ms. in duration. The electrodes were a pair of stainless steel needles inserted into the quadriceps muscles and fixed 5 mm apart. Seven days after gene delivery, the muscles were removed and subjected to analysis. Frozen muscle tissues were homogenized in ice-cold passive lysis buffer from Promega. The homogenate was centrifuged at 10,000 g for 10 min at 4°C. The supernatant was reserved for luciferase assay using Promega's dual luciferase assay kit. The luciferase activity was calculated as the ratio of firefly to Renilla (internal control) luciferase activity and represented as the average of triplicate experiments.

Computer-based DNA sequence motif search

We used MATCH software [18] (BIOBASE GmbH, Wolfenbuettel, Germany) to investigate transcriptional binding sites in the mouse *Glut1* promoter. We investigated mouse genome in the region of -1500 to +100 relative to transcription start of *Glut1* (Chr.4 11878131(+)).

cDNA microarray analysis

RNA was isolated from the skeletal muscle of sex- and age-matched RXRγ mice (line 4-3) and non-transgenic control mice

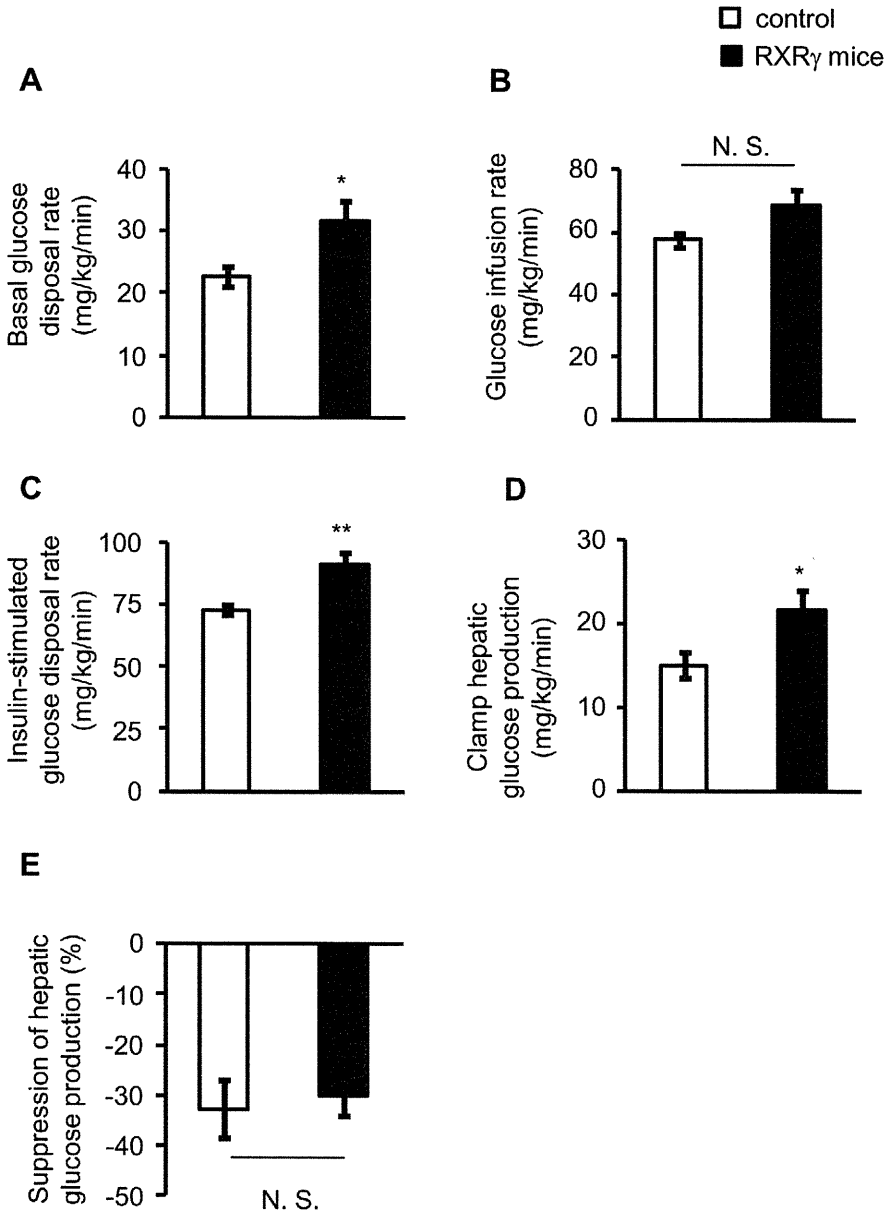

Figure 3. Hyperinsulinemic-euglycemic clamp test in RXRγ mice, fed a chow diet. (*A*) Basal glucose disposal rate, (*B*) glucose infusion rate needed to maintain euglycemia, (*C*) insulin-stimulated glucose disposal rate and (*D*) clamp hepatic glucose production (hepatic glucose production during the clamp period) (*E*) suppression of hepatic glucose production during the clamp period in RXRγ mice. Male mice, 13~16 weeks of age, were used. The number of animals used was 6 for control mice (open bars) and 7 for RXRγ mice (filled bars). * $P<0.05$ and ** $P<0.01$ compared with respective control. N. S., not significant.
doi:10.1371/journal.pone.0020467.g003

(females at 4 months of age, five samples from each group were combined). Each of the combined samples was hybridized to the Affymetrix MG430 microarray, which contains 45,102 genes, including expressed sequence tags (ESTs), and analyzed with the software Affymetrix Gene Chip 3.1. Of the 45,102 genes including ESTs analyzed, 8,054 (non-transgenic control mice) and 8,083 (transgenic) were expressed at a substantial level (absolute call is present and average difference is above 150). In order of fold changes in gene expression levels in skeletal muscle from RXRγ mice relative to control mice, genes whose expression was increased more than $2^{0.4}$-fold in RXRγ mice were listed (Dataset S1). Fold changes were calculated as an indication of the relative change of each transcript represented on the probe array. Differentially expressed genes were identified using the following criteria; 'absolute call' is present, and 'average difference' was above 250. 'Absolute call', which was calculated with this software using several markers, is an indicator of the presence or absence of each gene transcript. The 'average difference' value is a marker of the abundance of each gene, obtained by comparing the intensity of hybridization to 20 sets of perfectly matched 25-mer oligonucleotides relative to 20 sets of mismatched oligonucleotides using Affymetrix Gene Chip 3.1 software. All data of microarray is MIAME compliant and that the raw data has been deposited in a MIAME compliant database (GEO), whose accession number is GSE28448.

Gene Ontology Analysis

We used DAVID v6.7 [19] for gene ontology (GO) analysis. DAVID is a web application providing a comprehensive set of functional annotation tools to understand the biological meaning behind a large list of genes. Functional Annotation Clustering of DAVID was applied to the genes whose gene expression increased in RXRγ mice. Our GO analysis produced 62 GO terms from gene sets from RXRγ mice with increased expression compared to the wild-type mice, under the condition of $P<0.05$ (P value from Fisher's Exact Test). The obtained GO terms contained many similar functional concepts. In order to group similar GO terms, we applied the Functional Annotation Clustering tool provided by DAVID [19,20]. Twenty-three clusters were produced with genes showing increased expression. We showed one GO term of the lowest P value of all the members of an individual cluster.

Transcriptional factor binding sites analysis

We used MATCH software [18] with BKL TRANSFAC 2010.3 Release (BIOBASE GmbH, Worfenbuettel, Germany) to investigate transcriptional binding sites in the promoter regions of genes. The F-Match algorithm compares the number of sites found in a query sequence set against the background set. It is assumed, if a certain transcription factor (or factor family), alone or as a part of a *cis*-regulatory module, plays a significant role in the regulation of the considered set of promoters, then the frequency of the corresponding sites found in these sequences should be significantly higher than expected by random chance. We investigated the mouse genome in the region of -1000 to +100 relative to the transcription start of an individual gene. Statistical hypothesis testing was evaluated against housekeeping genes of mice. We investigated promoter regions of 15 genes: that is 14 'glucose metabolic process' genes with increased expression in RXRγ mice, plus Glut1. In the GO analysis, Glut1 was categorized as a 'transporter' not 'glucose metabolic process' gene.

Statistical analysis

Statistical analysis was performed using the Student's t test and analysis of variance (ANOVA) followed by Scheffe's test. Data were expressed as the mean ± SE. $P<0.05$ was considered statistically significant.

Results

Increased glucose metabolism in RXRγ mice

In our previous study, we established two lines of RXRγ mice (named lines 4-3 and 5-3) with similar expression levels of the *RXRγ* transgene and protein specifically in the skeletal muscle [9]. There was no significant difference in body weight, adipose tissue,

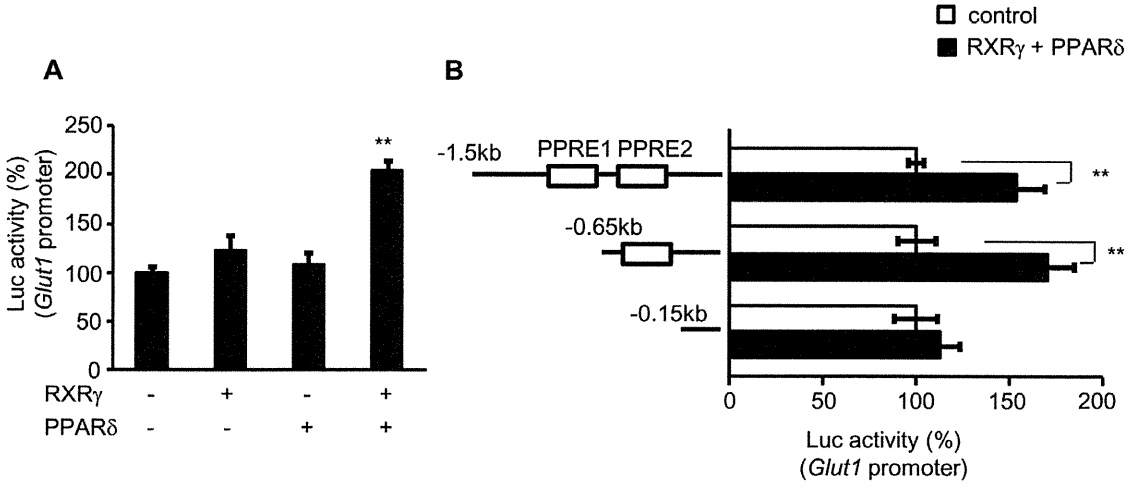

Figure 4. Transient transfection-reporter assay of the effect of RXRγ on *Glut1* promoter. (*A*) *Glut1*-Luc plasmid, with or without RXRγ and/or PPARδ expression vectors, was transfected into the quadriceps muscle of C57BL6 mice. Activation of the luciferase reporter gene was measured in relative light units and normalized to dual luciferase activity. Mean values from experiments (n = 5) are shown as fold induction, where the activity in the absence of RXRγ is the reference value (set at 100). (*B*) Schematic representations of serial deletion of *Glut1* promoter constructs are shown in the figure. Squares denote the putative PPAR/RXR binding sites. Open bars; *Glut1*-Luc without RXRγ and PPARδ expression vectors, and filled bars; *Glut1*-Luc with RXRγ and PPARδ expression vectors. The activity in the absence of RXRγ and PPARδ in each experiment for different *Glut1*-Luc construct in the reference value (set at 100). ** $P<0.01$, compared with the value of wild-type promoter in the absence of RXRγ/PPARδ.
doi:10.1371/journal.pone.0020467.g004

and liver weight between RXRγ and control mice in both lines 4-3 and 5-3, although the skeletal muscle weight was slightly lower in RXRγ mice than in control mice (Tables 1 and 2). In this study, blood glucose in RXRγ mice was lower than in control mice (fasting state, $P<0.01$ in lines 4-3 and 5-3; basal state, $P<0.05$ in line 4-3 and $P=0.06$ in line 5-3), which is consistent with our previous report [9].

To elucidate the role of the skeletal muscle RXRγ in systemic glucose metabolism, we performed glucose and insulin tolerance tests in RXRγ mice. The glucose tolerance test revealed increased glucose disposal in RXRγ mice relative to control mice (Fig. 1*A*). On the other hand, there was no significant difference in the insulin-induced hypoglycemic response between genotypes (Fig. 1*B*). These observations suggest that RXRγ mice have a higher capacity for glucose disposal with no change in insulin sensitivity.

Increased Glut1 expression and glucose uptake in the skeletal muscle of RXRγ mice

As both lines of RXRγ mice showed increased glucose metabolism, for the following experiments, we only utilized the line 4-3 of RXRγ mice (hereafter just RXRγ mice). Interestingly, mRNA expression of *Glut1* was increased in the skeletal muscle from RXRγ mice relative to control mice ($P<0.01$), whereas that of *Glut4* was unchanged (Fig. 2*A*). We also observed that Glut1 is significantly increased in RXRγ mice at the protein level ($P<0.05$), with no significant difference in Glut4 between genotypes (Fig. 2*B*). Consistently, we also found increased glucose uptake in the skeletal muscle from RXRγ mice relative to control mice ($P<0.05$), which was not further enhanced in the presence of insulin (Fig. 2*C*). We also observed increased glucose glycogen content in the skeletal muscle from RXRγ mice relative to control mice ($P<0.05$, Fig. 2*D*).

Increased basal glucose disposal rate of RXRγ mice

To gain further insight into the glucose metabolism in RXRγ mice, we performed a hyperinsulinemic-euglycemic clamp study. Plasma insulin concentrations during the basal period were similar between genotypes (Table 3). The basal glucose disposal rate was significantly increased in RXRγ mice than in the controls ($P<0.05$, Fig. 3*A*), supporting that an insulin-independent increase in glucose uptake occurred, as observed in Fig. 2*C*. Meanwhile, we observed that the rate of glucose infusion needed to maintain euglycemia (glucose infusion rate) was similar between genotypes (Fig. 3*B*), which is consistent with the result of the insulin tolerance test (Fig. 1*B*). On the other hand, insulin-stimulated glucose disposal rate was higher in RXRγ mice than in the controls ($P<0.01$, Fig. 3*C*), which probably reflects the increased basal glucose disposal rate (Fig. 3*A*). Also, the clamp hepatic glucose production (hepatic glucose production during the clamp period) was higher in RXRγ mice than in the controls ($P<0.05$, Fig. 3*D*). Meanwhile, hepatic glucose production was similarly suppressed by insulin in both genotypes (Fig. 3*E*). Together, these data support the idea that Glut1, an insulin-independent glucose transporter, is involved in the increased glucose disposal in the skeletal muscle of RXRγ mice.

Activation of the *Glut1* promoter by combination of RXRγ and PPARδ in the skeletal muscle *in vivo*

To examine whether RXRγ directly activates mRNA expression of *Glut1*, we performed the *in vivo* luciferase reporter analysis

Table 4. Gene Ontology Analysis.

GO ID	GO Term	P value
GO:0060537	muscle tissue development	6.91E-05
GO:0006461	protein complex assembly	6.78E-05
GO:0008104	protein localization	1.18E-04
GO:0051146	striated muscle cell differentiation	6.06E-04
GO:0030334	regulation of cell migration	8.04E-04
GO:0006886	intracellular protein transport	0.002367379
GO:0019220	regulation of phosphate metabolic process	0.00312153
GO:0048514	blood vessel morphogenesis	0.00172443
GO:0045859	regulation of protein kinase activity	0.00563927
GO:0006915	apoptosis	0.007513423
GO:0006006	glucose metabolic process	0.002958786
GO:0006917	induction of apoptosis	0.005257921
GO:0042981	regulation of apoptosis	0.014518039
GO:0043066	negative regulation of apoptosis	0.022995692
GO:0006633	fatty acid biosynthetic process	0.012664127
GO:0032956	regulation of actin cytoskeleton organization	0.027565775
GO:0043388	positive regulation of DNA binding	0.021966247
GO:0006469	negative regulation of protein kinase activity	0.045894089
GO:0016477	cell migration	0.045248711
GO:0030521	androgen receptor signaling pathway	0.027402985
GO:0055003	cardiac myofibril assembly	0.020081231
GO:0000165	MAPKKK cascade	0.032045331
GO:0046825	regulation of protein export from nucleus	0.027402985

738 genes up-regulated in RXRγ mice compared with wild-type mice by microarray (Listed in Dataset S1) were classified into GO functional annotations, as described in Methods.
doi:10.1371/journal.pone.0020467.t004

Table 5. List of 'glucose metabolic process' genes.

Gene Symbol	Gene description
Atf3	Activating transcription factor 3
Bpgm	2-3-bisphosphoglycerate mutase
Dcxr	Dicarbonyl L-xylulose reductase
Fbp2	Fructose bisphosphatase 2
Gbe1	Glucan branching enzyme 1
Gpd1l	Glycerol-3-phosphate dehydrogenase 1-like
Gpi1	Glucose phosphate isomerase 1
Gys2	Glycogen synthase 2
Igf2	Insulin-like growth factor 2
Mat2b	Methionine adenosyltransferase II, beta
Nisch	Nischarin; an imidazoline receptor
Pdk1	Pyruvate dehydrogenase kinase isoenzyme 1
Pgam1	Phosphoglycerate mutase 1
Pgd	Phosphogluconate dehydrogenase
Pgm2l1	Phosphoglucomutase 2-like 1
Phkb	Phosphorylase kinase beta

Up-regulated genes in RXRγ mice in the microarray, classified as 'glucose metabolic process' genes by GO analysis, as described in Method. Genes are listed in alphabetic order of gene symbol. Glut1, which appeared in the up-regulated list in the microarray (Dataset S1), is not included in this list, as it was classified 'transporter' in the GO analysis.
doi:10.1371/journal.pone.0020467.t005

using *Glut1* promoter (*Glut1*-Luc). In this study, the activity of *Glut1*-Luc was marginally enhanced by RXRγ alone (Fig. 4*A*). Moreover, we found no significant activation of the *Glut1*-Luc by PPARδ, an important regulator of glucose as well as lipid metabolism in the skeletal muscle [7]. Interestingly, combination of RXRγ and PPARδ resulted in significant increase in *Glut1*-Luc activity in the skeletal muscle *in vivo* ($P<0.01$) (Fig. 4*A*). Motif search analysis revealed two putative PPAR-responsive elements (PPRE1 and PPRE2) (−657/−645 and −520/−508, respectively) in the mouse *Glut1* promoter. A series of deletion mutant analysis showed that combination of RXRγ and PPARδ activates the regions of −1500/+75, and −647/+75, but not the region of −152/+75 in the *Glut1* promoter (Fig. 4*B*), suggesting that the second putative PPRE (−520/−508) is involved in the RXRγ/PPARδ-induced *Glut1* promoter activation.

Microarray and bioinformatics analyses of up-regulated gene in RXRγ mice

In order to gain insight into the gene expression change in RXRγ mice, we performed microarray analysis. As shown in Dataset S1, 738 genes were up-regulated in the analysis. As expected, Glut1 expression was increased in the microarray data. Also, SREBP1c expression, which we previously reported [9], was increased in the microarray data. Using the data, we performed GO analysis to determine if genes, up-regulated in RXRγ mice, are associated with particular biological processes. Our GO analysis revealed genes with increased expression in the RXRγ mice in various categories (Table 4), including 'glucose metabolic process' genes and 'fatty acid biosynthetic process' genes, which indicated that overexpression of RXRγ affects the expression of many genes. The up-regulated genes categorized as glucose metabolism genes in GO term are listed in Table 5. Among them, we confirmed enhanced gene expression by quantitative real time PCR (Fig. 5), supporting the microarray data reliable. Moreover, we calculated the ratio of putative transcription factor binding motifs in glucose metabolism genes, which were up-regulated in RXRγ mice. In the sample, several motifs showed statistical significance (Table 6) ($P<0.05$), including PPAR responsive elements. These data suggest that glucose metabolism genes up-regulated in RXRγ mice are possible target genes of the RXRγ and PPAR heterodimer.

Discussion

RXRγ is a nuclear receptor-type transcription factor that is expressed abundantly in the skeletal muscle and is regulated by nutritional conditions. Treatment of obese and diabetic mice with RXR pan-agonists (agonists for all the RXR isoforms) has improved glucose metabolism in mice [21–23], suggesting the beneficial effect of RXR on diabetes. However, which RXR isoform(s) are involved and where they work to improve diabetes

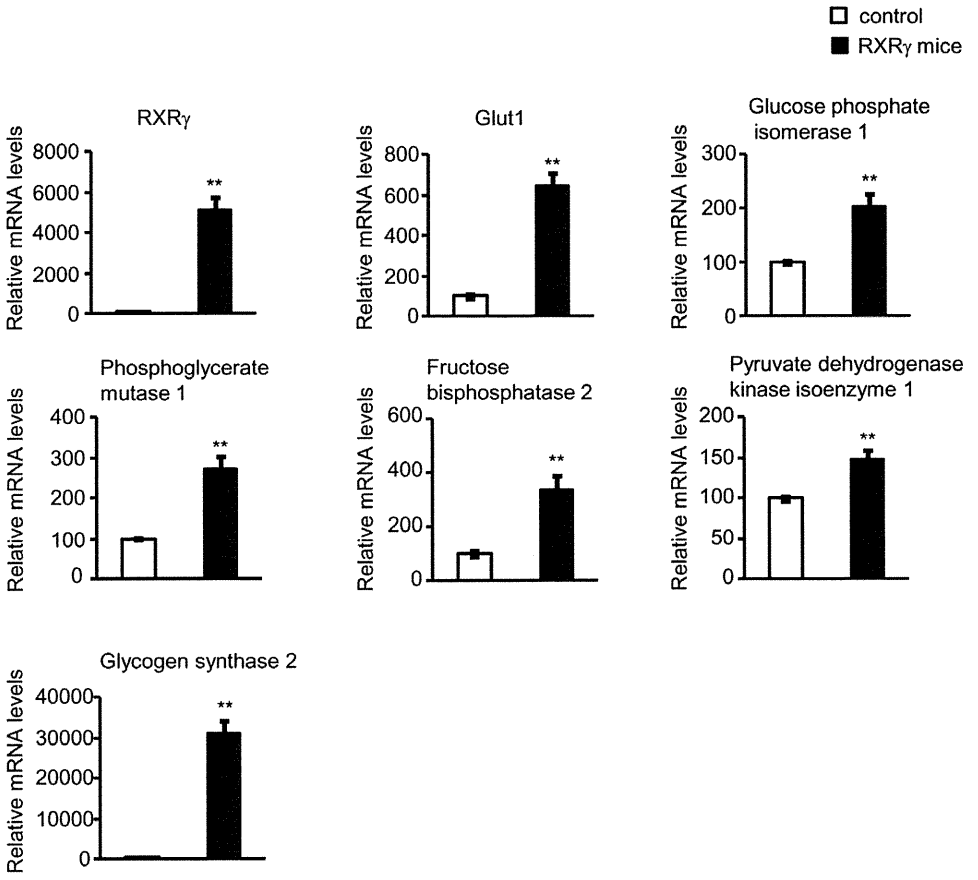

Figure 5. Levels of 'glucose metabolic process' gene expression in the skeletal muscle of RXRγ mice. Representative gene expressions of 'glucose metabolic process genes' analyzed by microarray and GO analysis (Table 5) were examined by quantitative real-time PCR. The value for wild-type (littermates of line 4-3) mice was set at 100, and relative values are shown. Mice were females of 4 months of age. The number of animals was 6 for both control (open bars) and RXRγ (filled bars) mice. These samples were also used in microarray analysis (Dataset S1). * $P<0.05$ and ** $P<0.01$ compared with respective control. N. S., not significant.
doi:10.1371/journal.pone.0020467.g005

Table 6. Possible transcription factor binding sites in the 'glucose metabolic process' gene up-regulated in RXRγ mice.

Transcription factors	Matrix name	P-value
WT1, WT1 -KTS, WT1 I, WT1 I -KTS	WT1_Q6	6.98E-04
HNF-4, HNF-4alpha	HNF4ALPHA_Q6	0.0013
PPARalpha	PPARA_01	0.0017
c-Myb, c-Myb-isoform1	VMYB_02	0.0026
PPARalpha, PPARdelta, PPARgamma	PPAR_DR1_Q2	0.003
CART1, CART1, CART1	CART1_01	0.0036
COUP-TF1, COUP-TF2, HNF-4, HNF-4alpha	COUP_DR1_Q6	0.0036
CP2, CP2-isoform1	CP2_02	0.0055
NRF1-isoform1, NRF1-isoform2, NRF1-xbb1	TCF11_01	0.0057
SZF1	SZF11_01	0.0057
PPARgamma	PPARG_01	0.0057
COUP-TF1, COUP-TF2, HNF-4, HNF-4alpha, HNF4gamma	DR1_Q3	0.0057
BRCA1, BRCA1	BRCA_01	0.0065
HNF-3beta	HNF3B_01	0.007
Pax-2b, pax2	PAX2_01	0.007
C/EBPalpha, C/EBPbeta(LAP), C/EBPbeta(p20), C/EBPbeta(p20), C/EBPbeta(p34), C/EBPbeta(p35), C/EBPgamma, cebpe, CRP3, NF-IL6-1, NF-IL6-3	CEBP_Q3	0.007
MITF, MITF-M1, tcfec, TFEA, TFEA-xbb1, TFEA-xbb2, tfeb, tfeb-isoform1	TFE_Q6	0.007
AP-2alpha, AP-2beta, AP-2gamma	AP2_Q6_01	0.0077
Pax-4a, Pax-4c, Pax-4d, Pax4	PAX4_04	0.0079
c-Myc, deltaMax, max, max-isoform1, max-isoform2, N-Myc	MYCMAX_03	0.0093

The mouse genome in the region of −1000 to +100 relative to the transcription start of an individual gene classified as glucose metabolism gene by GO analysis (Table 5), was analyzed. Statistical hypothesis testing was evaluated against housekeeping genes of mice. Matrics names are based on the MATCH software (see **Methods**), which are listed in *P*-value order. Indicated binding sites of transcription factors appeared significantly more frequent occurrence in the promoter sets.
doi:10.1371/journal.pone.0020467.t006

has not been addressed. Here, we investigated glucose metabolism in RXRγ mice.

We demonstrated increased glucose metabolism in RXRγ mice relative to control mice, although there was no significant difference in the insulin-induced hypoglycemic effect between genotypes, based on insulin tolerance test and glucose clamp analysis. Because insulin level is similar between RXRγ mice and control mice, it is unlikely that increased insulin secretion is responsible for increased glucose tolerance in RXRγ mice. On the other hand, mRNA and protein expression of Glut1 is increased in the skeletal muscle from RXRγ mice relative to control mice, with increased glucose uptake and glycogen content. Because transgenic overexpression of Glut1 in the skeletal muscle has resulted in increased glucose uptake [24], glycogen content [25] and lowering of blood glucose [24], it is likely that enhanced glucose tolerance in RXRγ mice is mediated at least in part by increased Glut1 in the skeletal muscle.

As RXRγ is a nuclear receptor-type transcription factor that heterodimerizes with many nuclear receptors [6], we examined whether the *Glut1* gene is directly regulated by RXRγ. In an *in vivo* luciferase reporter analysis, combination of RXRγ and PPARδ activates the *Glut1* promoter activity, which is diminished by deletion of the putative PPREs. It is, therefore, RXRγ/PPARδ may activate *Glut1* expression in the skeletal muscle *in vivo*. In this regard, we found that overexpression of RXRγ or PPARδ alone or both in C2C12 myocytes *in vitro* does not induce *Glut1* gene expression (unpublished data). This may be because C2C12 cells lack other factor(s) that are present in the skeletal muscle *in vitro* and are required to activate *Glut1* transcription. Whether the increased *Glut1* gene in RXRγ mice is mediated by RXRγ/PPARδ should be confirmed by additional experiments using PPARδ knockout mice. Meanwhile, the transgene expression level in RXRγ mice was very high, and appeared to be beyond the physiological level. Nonetheless, if RXRγ can be enhanced in skeletal muscle, an increase in glucose metabolism can be expected.

We recently demonstrated that in addition to glycogen content, RXRγ mice exhibit increased triglyceride in the skeletal muscle as a result of increased SREBP1c gene expression [9]. In obese and diabetic subjects, intramuscular lipid is high with insulin resistance [26]. Moreover, in athletes, the skeletal muscle is also high in lipid but with high insulin sensitivity, which is known as the athlete paradox [27,28]. A partial explanation is an increased fatty acid load in obese and diabetic subjects, but not in athletes; increased intramuscular lipotoxic fatty acid metabolites, such as diacylglycerol and ceramide, cause insulin resistance in skeletal muscles [29,30]. Taken together with our previous report [9], this study demonstrates that RXRγ mice do not develop insulin resistance despite high intramuscular lipids, and appear to be protected against obesity-induced lipotoxicity in the skeletal muscle. Depositing glucose as both glycogen and triglycerides in the skeletal muscle may be effective in enhancing glucose metabolism.

Microarray analysis showed that various genes are up-regulated in the skeletal muscle of RXRγ mice. As RXRγ can heterodimerize several nuclear receptors, it is not surprising that expression of many genes was up-regulated by RXRγ overexpression. Concerning glucose metabolism genes, in the skeletal muscle of RXRγ mice, the expression levels of genes, such as glucose phosphate isomerase 1 and phosphoglycerate mutase 1 (stimulate glycolysis or gluconeogenesis), fructose bisphosphatase 2 (stimulates gluconeogenesis), pyruvate dehydrogenase kinase

isoenzyme 1 (suppresses glycolysis), glycogen synthase 2 (stimulates glycogen synthesis)[31,32], were markedly increased (Fig. 5), suggesting the anabolic reaction of glucose. This is consistent with the observation that the glycogen content of skeletal muscle is higher in RXRγ mice (Fig. 2C). It is of note that glycogen synthase 2 is a liver-type enzyme, not a skeletal muscle-type enzyme [32]. In addition, usually, gluconeogenesis is not considered to be a major metabolic pathway in skeletal muscle. Chronic transgenic overexpression of RXRγ may have caused a super-physiological gene expression change in the skeletal muscle. Meanwhile, our bioinformatics analysis showed that glucose metabolism genes up-regulated in RXRγ mice contain several transcription factor binding motifs including PPRE in their promoter region. These observations support the concept that the RXRγ/PPAR heterodimer contributes to activation of these gene sets, although this needs to be confirmed by further experiments.

In summary, we demonstrated enhanced glucose metabolism with increased Glut1 expression and glucose uptake in RXRγ mice. This study suggested that activation of the skeletal muscle RXRγ is a novel therapeutic strategy to treat or prevent type 2 diabetes.

Supporting Information

Dataset S1 List of genes up-regulated in RXRγ mice compared with wild-type control mice by microarray. (XLS)

Acknowledgments

We thank Dr. Christopher K. Glass (University of California, San Diego) for discussion. We thank Dr. Kotaro Ishibashi (Daiichi-Sankyo Co., Ltd.) for assistance in animal experiments.

Author Contributions

Conceived and designed the experiments: JIO KN SS YK OE YO. Performed the experiments: SS YK FA TS SK (Sayaka Kanai) MH YM NF TTI MT HA TY HK (Hideki Katagiri) SK (Saori Kakehi) YT HK (Hideo Kubo) SM. Analyzed the data: SS YK FA TS SK (Sayaka Kanai) MH YM NF TTI HA TY HK (Hideki Katagiri) SK (Saori Kakehi) YT HK (Hideo Kubo) SM. Contributed reagents/materials/analysis tools: TTI HA JIO KN. Wrote the paper: SS YK OE YO.

References

1. Zurlo F, Larson K, Bogardus C, Ravussin E (1990) Skeletal muscle metabolism is a major determinant of resting energy expenditure. J Clin Invest 86: 1423–1427.
2. DeFronzo RA (1988) Lilly lecture 1987. The triumvirate: beta-cell, muscle, liver. A collusion responsible for NIDDM. Diabetes 37: 667–687.
3. Marshall BA, Hansen PA, Ensor NJ, Ogden MA, Mueckler M (1999) GLUT-1 or GLUT-4 transgenes in obese mice improve glucose tolerance but do not prevent insulin resistance. Am J Physiol 276: E390–E400.
4. Petersen KF, Dufour S, Savage DB, Bilz S, Solomon G, et al. (2007) The role of skeletal muscle insulin resistance in the pathogenesis of the metabolic syndrome. Proc Natl Acad Sci U S A 104: 12587–12594.
5. Kim JK, Zisman A, Fillmore JJ, Peroni OD, Kotani K, et al. (2001) Glucose toxicity and the development of diabetes in mice with muscle-specific inactivation of GLUT4. J Clin Invest 108: 153–160.
6. Shulman AI, Mangelsdorf DJ (2005) Retinoid x receptor heterodimers in the metabolic syndrome. N Engl J Med 353: 604–615.
7. Lee CH, Olson P, Hevener A, Mehl I, Chong LW, et al. (2006) PPARdelta regulates glucose metabolism and insulin sensitivity. Proc Natl Acad Sci U S A 103: 3444–3449.
8. Szanto A, Narkar V, Shen Q, Uray IP, Davies PJ, et al. (2004) Retinoid X receptors: X-ploring their (patho)physiological functions. Cell Death Differ 11: S126–S143.
9. Kamei Y, Miura S, Suganami T, Akaike F, Kanai S, et al. (2008) Regulation of SREBP1c gene expression in skeletal muscle: role of retinoid X receptor/liver X receptor and forkhead-O1 transcription factor. Endocrinology 149: 2293–2305.
10. Suzuki R, Tobe K, Aoyama M, Inoue A, Sakamoto K, et al. (2004) Both insulin signaling defects in the liver and obesity contribute to insulin resistance and cause diabetes in Irs2(-/-) mice. J Biol Chem 279: 25039–25049.
11. Uno K, Katagiri H, Yamada T, Ishigaki Y, Ogihara T, et al. (2006) Neuronal pathway from the liver modulates energy expenditure and systemic insulin sensitivity. Science 312: 1656–1659.
12. Erion DM, Yonemitsu S, Nie Y, Nagai Y, Gillum MP, et al. (2009) SirT1 knockdown in liver decreases basal hepatic glucose production and increases hepatic insulin responsiveness in diabetic rats. Proc Natl Acad Sci U S A 106: 11288–11293.
13. Tanaka S, Hayashi T, Toyoda T, Hamada T, Shimizu Y, et al. (2007) High-fat diet impairs the effects of a single bout of endurance exercise on glucose transport and insulin sensitivity in rat skeletal muscle. Metabolism 56: 1719–1728.
14. Ito A, Suganami T, Miyamoto Y, Yoshimasa Y, Takeya M, et al. (2007) Role of MAPK phosphatase-1 in the induction of monocyte chemoattractant protein-1 during the course of adipocyte hypertrophy. J Biol Chem 282: 25445–25452.
15. Fujii N, Ho RC, Manabe Y, Jessen N, Toyoda T, et al. (2008) Ablation of AMP-activated protein kinase alpha2 activity exacerbates insulin resistance induced by high-fat feeding of mice. Diabetes 57: 2958–2966.
16. Lowry OH, Passonneau JV (1972) A flexible system of enzymatic analysis. Academic Press London 1-291.
17. Aihara H, Miyazaki J (1998) Gene transfer into muscle by electroporation in vivo. Nat Biotechnol 16: 867–870.
18. Kel AE, Gossling E, Reuter I, Cheremushkin E, Kel-Margoulis OV, et al. (2003) MATCH: A tool for searching transcription factor binding sites in DNA sequences. Nucleic Acids Res 31: 3576–3579.
19. Huang da W, Sherman BT, Lempicki RA (2009) Systematic and integrative analysis of large gene lists using DAVID bioinformatics resources. Nat Protoc 4: 44–57.
20. Carbon S, Ireland A, Mungall CJ, Shu S, Marshall B, Lewis S (2009) AmiGO: online access to ontology and annotation data. Bioinformatics 25: 288–289.
21. Mukherjee R, Davies PJ, Crombie DL, Bischoff ED, Cesario RM, et al. (1997) Sensitization of diabetic and obese mice to insulin by retinoid X receptor agonists. Nature 386: 407–410.
22. Davies PJ, Berry SA, Shipley GL, Eckel RH, Hennuyer N, et al. (2001) Metabolic effects of rexinoids: tissue-specific regulation of lipoprotein lipase activity. Mol Pharmacol 59: 170–176.
23. Shen Q, Cline GW, Shulman GI, Leibowitz MD, Davies PJ (2004) Effects of rexinoids on glucose transport and insulin-mediated signaling in skeletal muscles of diabetic (db/db) mice. J Biol Chem 279: 19721–19731.
24. Marshall BA, Ren JM, Johnson DW, Gibbs EM, Lillquist JS, et al. (1993) Germline manipulation of glucose homeostasis via alteration of glucose transporter levels in skeletal muscle. J Biol Chem 268: 18442–18445.
25. Ren JM, Marshall BA, Gulve EA, Gao J, Johnson DW, et al. (1993) Evidence from transgenic mice that glucose transport is rate-limiting for glycogen deposition and glycolysis in skeletal muscle. J Biol Chem 268: 16113–16115.
26. Goodpaster BH, Wolf D (2004) Skeletal muscle lipid accumulation in obesity, insulin resistance, and type 2 diabetes. Pediatr Diabetes 5: 219–226.
27. Stannard SR, Johnson NA (2004) Insulin resistance and elevated triglyceride in muscle: more important for survival than "thrifty" genes? J Physiol 554: 595–607.
28. Goodpaster BH, He J, Watkins S, Kelley DE (2001) Skeletal muscle lipid content and insulin resistance: evidence for a paradox in endurance-trained athletes. J Clin Endocrinol Metab 86: 5755–5761.
29. Schenk S, Horowitz JF (2007) Acute exercise increases triglyceride synthesis in skeletal muscle and prevents fatty acid-induced insulin resistance. J Clin Invest 117: 1690–1698.
30. Liu L, Zhang Y, Chen N, Shi X, Tsang B, et al. (2007) Upregulation of myocellular DGAT1 augments triglyceride synthesis in skeletal muscle and protects against fat-induced insulin resistance. J Clin Invest 117: 1679–1689.
31. Kaslow HR, Lesikar DD, Antwi D, Tan AW (1985) L-type glycogen synthase. Tissue distribution and electrophoretic mobility. J Biol Chem 260: 9953–9956.
32. Salway JG (1999) Metabolism at a glance. London: Blackwell Science Ltd.

Circulation
JOURNAL OF THE AMERICAN HEART ASSOCIATION

American Heart Association®
Learn and Live℠

Involvement of Endoplasmic Stress Protein C/EBP Homologous Protein in Arteriosclerosis Acceleration With Augmented Biological Stress Responses

Junhong Gao, Yasushi Ishigaki, Tetsuya Yamada, Keiichi Kondo, Suguru Yamaguchi, Junta Imai, Kenji Uno, Yutaka Hasegawa, Shojiro Sawada, Hisamitsu Ishihara, Seiichi Oyadomari, Masataka Mori, Yoshitomo Oka and Hideki Katagiri

Circulation published online August 1, 2011
Circulation is published by the American Heart Association. 7272 Greenville Avenue, Dallas, TX 72514
 Print ISSN: 0009-7322. Online ISSN: 1524-4539